

3-14-1985

Near Edge Fine Structures on Electron Energy Loss Spectroscopy Core Loss Edges


C. Colliex
Université Paris-Sud

T. Manoubi
Université Paris-Sud

M. Gasgnier
C.N.R.S.

L. M. Brown
Cambridge

Follow this and additional works at: <https://digitalcommons.usu.edu/electron>

 Part of the [Biology Commons](#)

Recommended Citation

Colliex, C.; Manoubi, T.; Gasgnier, M.; and Brown, L. M. (1985) "Near Edge Fine Structures on Electron Energy Loss Spectroscopy Core Loss Edges," *Scanning Electron Microscopy*. Vol. 1985 : No. 2 , Article 3. Available at: <https://digitalcommons.usu.edu/electron/vol1985/iss2/3>

This Article is brought to you for free and open access by the Western Dairy Center at DigitalCommons@USU. It has been accepted for inclusion in Scanning Electron Microscopy by an authorized administrator of DigitalCommons@USU. For more information, please contact digitalcommons@usu.edu.



NEAR EDGE FINE STRUCTURES ON ELECTRON ENERGY LOSS SPECTROSCOPY CORE LOSS EDGES

C. Colliex¹, T. Manoubi¹, M. Gasgnier², L.M. Brown³

¹ Laboratoire de Physique des Solides, associé au CNRS
Bât. 510, Université Paris-Sud, 91405 - Orsay (France)

² Permanent address : ERA 210, C.N.R.S., Bellevue

³ Metal Physics Dept., Cavendish Lab., Cambridge CB3 0HE (G.B.)

(Paper received April 16 1984, Completed manuscript received March 14 1985)

Abstract

Core edges recorded in Electron Energy Loss Spectroscopy (EELS) display a large variety of profiles. We have investigated several specific aspects concerning Energy Loss Near Edge Structures (ELNES) and emphasize the interest in a careful edge shape analysis to obtain refined microanalytical information, such as local symmetry. After indicating the general impact of EELS fine structures as compared to EDX and Auger spectroscopies we discuss the instrumental conditions required for recording satisfactory spectra and consider the theoretical problems which are involved in data interpretation. The major portion of this paper presents results for selected K, L₂₃, M₄₅ and N₄₅ core excitations in compounds (mainly oxides). In each case the phenomena governing the ELNES distribution are pointed out. In conclusion, we summarize the potential of a careful analysis of ELNES for studying the chemical state of the absorbing atom and the symmetry of its first coordination shell (molecular description) or longer range effects (projections of solid state density of states as seen by the ejected atom).

Keywords : Microanalytical information
Electron energy loss spectroscopy
Core loss edge shape
Atomic point of view in a solid
Local density of states
Multielectron effects

Address for correspondence :

C. Colliex
Laboratoire de Physique des Solides
Bât. 510, Université Paris-Sud
91405 Orsay Cédex (France) Phone (6) 941.53.70

Importance of fine structure in different types of analytical signals

In the general environment of an electron microscope column, several techniques have been recently developed to combine morphological observation, structural characterization and chemical analysis of specimen areas of one to several nanometers typical extension. A new generation of instruments, generally named "analytical electron microscopes", is the result of such an association of spectroscopic devices for electron energy loss (EELS), energy dispersive X-ray (EDX) and Auger emission spectroscopies (AES).

However, "analysis" refers to several types of information content. In its simple meaning, chemical analysis consists in recognizing a given element present within the analysed volume. But it can also concern more elaborate types of information, such as the valence state of the element (doubly or triply ionized), the environmental symmetry of its site (tetrahedral or octahedral..) or its short or long range surroundings (Colliex, 1984b).

In all analytical modes considered in this paper, the useful information is derived from an interaction process between the incident electron and a target electron lying originally on a core orbital (C). EELS investigates the excitation mechanisms between a core level and an unoccupied state (U) lying above the Fermi level E_F : it is a spectroscopy of type CU - see Fig. 1a. The relevant signal is an edge, superposed over a decreasing background, which can be displayed as in Fig. 2 after background stripping. An average jump ratio at the edge is of the order of one to several units depending on the edge under consideration. For comparison, Fig. 1b and Fig. 1c represent in a similar diagram the levels involved in EDX and AES spectroscopies : they both result from a de-excitation process in which a higher lying electron originating from a core C or a valence band V level fills the hole produced by the primary process. The first case can be called CC spectroscopy and the second CCV or CVV depending on the type of levels involved in the decay transition. An EDX spectrum consists in lines superposed over a background of weaker intensity (average S/B ratio 10 to 50), and an Auger spectrum is made of lines or bands on a background with typical S/B ratios of

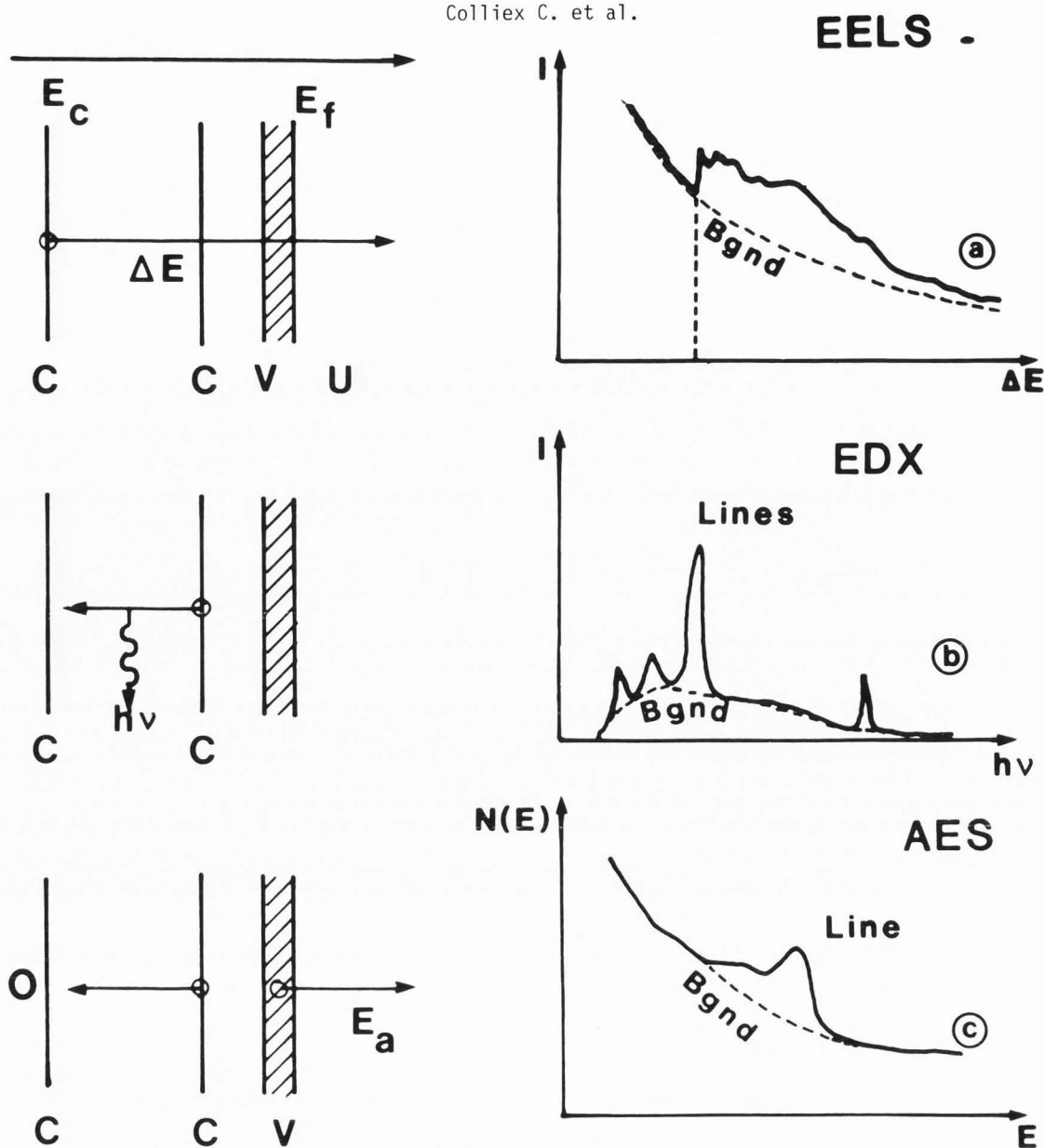


Fig. 1 - Definition of the spectroscopies (EELS, EDX and AES) used in analytical electron microscopy. Illustration of the general shape for the signal and background in each case.

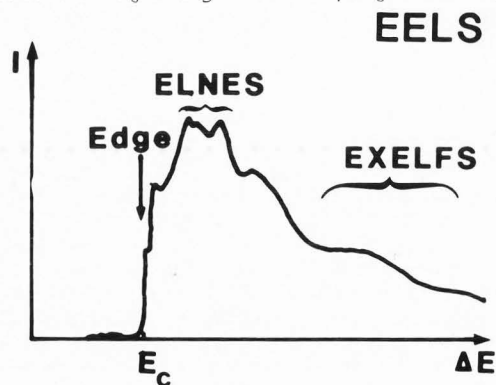


Fig. 2 - Typical EELS edge after background stripping pointing out the major features of fine structures.

the order of 1, similarly to EELS case. Detailed analytical information is conveyed in several ways. In an X-ray emission spectrum, the lines corresponding to electronic transitions between core levels may exhibit chemical shifts when the oxidation state or the nature of ligands is changed. The observed shifts (Lüger, 1971) are however of the order of a few eV or less and their detection requires a high resolution wavelength dispersive X-ray (WDX) analyser. For the standard EDX technique based on energy dispersion in a solid-state detector the energy resolution is too poor to reveal such changes.

More interesting are the Auger and EELS cases because a lineshape or edgeshape analysis can provide much more information about the specimen. Consider the situation in AES, as reviewed recently by Madden (1983). For a long time AES studies

have concentrated on elemental analysis by identification of the energy position of peaks in derivative Auger spectra. Actually early work by Lander (1953) had clearly stated that AES could be used as a valence band spectroscopy if the shape of the Auger (CCV or CVV) lines recorded in integral mode were properly analysed. A useful approach developed during the last few years is to analyze a CVV line in terms of the sum of convolution products of independent-particle valence band density of states (DOS) components. This method has been successful for a few simple metals. However some CVV Auger spectra from surfaces exhibit lineshapes which bear no simple relationship with convolution products of DOS distributions; they can be termed "atomic-like" or "quasi-atomic" because they contain features too narrow to be interpreted by band density of states. The specific case of compound surfaces has been the subject of recent discussions (Citrin et al., 1976, Fuggle, 1981) which point out the possibility of interatomic transitions in which the valence electrons taking part in the Auger decay come not from the site on which the initial core hole was produced but from neighbouring sites. Such interpretative studies have therefore introduced a new dimension to Auger spectroscopy, in which one tries to extract local bonding information from detailed analysis of the relevant valence band features.

Finally, one might underline the potential importance of deriving local bonding information in solid state physics or science of materials. A classic example is the presence of embrittling layers of elements segregated to grain boundaries, where the local environment of an atom at the boundary plays a crucial role in the mechanical behaviour of the material.

Position of the problem in EELS.

Back to EELS spectroscopy, the historical story is very similar to AES. Early core-edge studies noted the close similarity of structures following characteristic edges in EELS or X-ray absorption spectra, and plots of the density of states in the unoccupied part of the conduction band (Colliex and Jouffrey, 1972). During the past decade, much more attention has been paid to the development of a quantitative micro-analytical technique, for which the state of the art is reviewed by Egerton (1984). Over the last few years, however, interest in near edge fine structures has been renewed, stimulated by two general trends: 1) improvement in spectrometer technologies which combine good energy resolution (< 1 eV) with the high collection efficiency necessary for studying core-loss edges in the energy loss range 200-2000 eV (Krivanek and Swann, 1981, Jeanguillaume et al., 1982); 2) also there is increased interest in the near edge fine structures measured by synchrotron X-ray absorption spectroscopy and associated interpretative efforts by various groups of theoreticians. It is important to note that the extraction of fine structure information from focused electron probes demands a specimen particularly resistant to radiation damage, and that radiation damage is one of the major barriers

to the study of organic materials.

Recent review papers by Colliex (1984a) and Egerton (1983) have summarized the major contributions to the fine structure in a core-loss (or absorption) edge, which can be used to extract detailed information. The general shape of an edge is determined by atomic considerations. It depends on the symmetry of the orbitals (initial and final) which obey the well known dipole selection rules for electronic transitions:

$$l' - l = \Delta l = \pm 1 \quad (1)$$

Colliex (1984a) contains a tabulation of all edges of interest for pure elements in the energy range ≈ 30 eV to ≈ 2500 eV, classified into five main families of edge shapes as shown in Fig. 3:

- a) saw-tooth profile such as calculated in the hydrogenic model;
- b) delayed edge with a relatively large transfer of oscillator strength to higher energies, as a consequence of an effective centrifugal barrier most important for final states of large l' quantum number;
- c) "white-lines" narrow and intense peaks, often exhibiting the spin-orbit splitting of the initial level;
- d) "plasmon-like" resonance peak for edges associated with intense oscillator strengths in the low energy loss range;
- e) mixed profile combining a discrete transition to a bound state at threshold and a delayed contribution to continuum states at energies far above threshold.

These general shapes can be understood upon a close examination of the electronic configuration of each element. The only important edges are those corresponding to an initial state of maximum occupied l for a given n shell because these have the maximum cross-section. It is however very difficult to record experimental atomic spectra; the specimens usually consist of molecular or solid state assemblies of one or several types of atoms (compounds). The observed edges display much more complex structures than those discussed in simplified atomic terms. Moreover, the detailed profiles depend on the allotropic variety or compound in which the element is found. Recent important systematic studies have been made to obtain complete libraries of spectra (Zaluzec, 1982, Ahn and Krivanek, 1982). Many comparative studies can be extracted from such atlases. The various spectral modifications induced by the local solid state environment affect (see Figure 2):

- 1) the threshold: variation of the position, of the slope and of the associated fine structures. For a long time, the displacement of an edge has been known as a "chemical shift" in which one measures the translation along the energy scale of edges with constant profile. This approach is often a consequence of a rather poor energy resolution which averages features at the edge, so that one

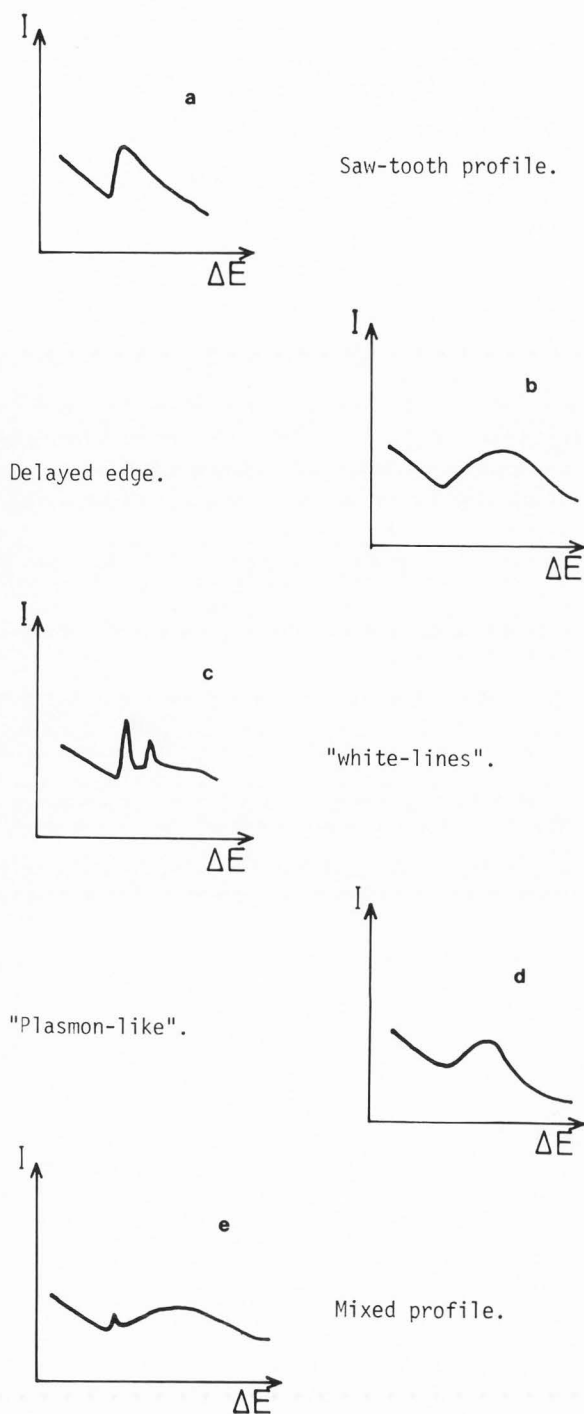


Fig. 3 - Schematic representation of the five main families of edge shape introduced in the text.

detects only shifts in energy without noticing modifications in the edge shape.

- 2) "near-edge" structures : appearing in an energy loss range extending from typically 10 to 50 eV above the edge. The acronym XANES for X-ray absorption near edge structure has been used in the recent literature concerning similar

structures in X-ray absorption spectra and ELNES has been suggested by Colliex (1982) and Taftø and Zhu (1982) to identify these features in EELS spectra. They have been mostly interpreted in terms of the conduction band density of states (DOS) and are complementary to the valence band DOS already mentioned for Auger lineshapes interpretation.

- 3) "extended" oscillations : superposed on the decreasing tail of the core loss edge. The equivalent extended X-ray absorption fine structures (EXAFS) are now well understood and used for solving short range environment problems in many substances (Lee et al., 1981). They cover typically several hundreds of eV above the edge and their EELS equivalent are generally termed EXELFS following the original work (Ritsko et al., 1974, Leapman and Cosslett, 1976 and Colliex et al., 1976). EXELFS spectra have been published by many authors during the last few years (Kincaid et al., 1978, Disko et al., 1982, Leapman, 1982) and reviews can be found in the papers of Leapman et al., (1981) and of Csillag et al. (1981). EXELFS can be analyzed in the same way as EXAFS by use of the formulation developed by Ashley and Doniach (1975) and Lee and Pendry (1975) after the pioneering contribution due to Sayers et al. (1971).

For several reasons, the potential field of application of EXELFS appears limited. By comparison with EXAFS studies, it offers a clear advantage because it is easily used for light elements and because it can be applied to very small volumes of material which can be characterized by other electron microscopy techniques (Batson and Craven, 1979, Batson et al., (1980). However the fine structure modulations on the tail of a characteristic signal are weak and superposed on an intense background. Consequently very high counting rates are required to offer a satisfactory signal of noise ratio. A second limit is due to the fact that in EELS the edges lie in the moderate 1000 eV energy loss range, in which the EXELFS from one edge often overlap another edge. The accuracy of the procedure used for the estimation of nearest neighbour distances is defined by the overall energy loss domain over which the Fourier analysis of oscillations is performed. In the EXELFS situations, the low k truncation is determined by the necessity of avoiding multiple scattering events close to the edge while the high k truncation is imposed either by the onset of another edge or by noise. Altogether this restricted k-window degrades the capability of the method to solve local order problems. A last point worth mentioning is that the required theory is not fully developed for situations involving more complex edges (e.g. M_{23} , M_{45} ..) which are clearly observable in EEL spectra, and for cases departing from the dipolar approximation when large collection angles are used.

Because of the limitations just discussed, we think that a more detailed study of the features classified above as 1) and 2) is rather promising because it is easier to acquire spectra with an acceptable signal to noise ratio. The remainder of this paper describes a selection of

examples of experimental recording of near edge fine structures together with the theoretical problems involved in their interpretation.

Instrumental parameters

The experimental work was performed with the Scanning Transmission Electron Microscope (STEM) Vacuum Generators VG HB501 operated at Orsay over the past three years. Details concerning its main modes of operation for imaging and analytical purposes have been described elsewhere (Colliex and Trebbia, 1982, Colliex and Treacy, 1983, Colliex and Mory, 1983). Hence we need only summarize the major characteristics pertinent to the recording and study of near edge structures in EELS.

The STEM configuration delivers on the thin foil specimen a convergent beam of electrons within a probe of very small size d : the angle of illumination α_0 governs the dimension and the shape of the distribution of primary electrons on the specimen entrance surface. In our system, 70 % of the incident current is contained within a circle of radius $r \approx 0.3$ nm for $\alpha_0 = 7.5$ mrad and ≈ 2 nm for $\alpha_0 = 15.0$ mrad, these two conditions being the commonly used ones. The analysed volume can roughly be described as a cylinder of section set by the primary beam and of height imposed by the specimen thickness, as long as it remains sufficiently thin to maintain the beam spread at a reasonable level. In most cases, the specimen properties are monitored by standard imaging and diffraction, so that a homogeneous area can be chosen within a characterised specimen grain size, and repeatedly scanned during the recording of spectra. In most cases, the acquisition area consists of a rectangular raster of several nanometers on a side.

The spectrometer is a Gatan 607 homogeneous field magnetic sector, whose design compensates for second order aberrations. It has proven to be capable of achieving an energy resolution of the order of 1 eV on characteristic edges while collecting all electrons inelastically scattered within a collection angle $\beta_0 \approx 25$ mrad at the specimen exit surface. Spectra shown below illustrate this typical performance level.

The spectra are recorded in a sequential mode, that is, an externally driven magnet current scans them in front of the selection slit and the detector located behind them. A computer is used to govern the conditions of spectrum acquisition by applying a step function ramp on the magnet current. It also collects in a digital format the signals coming from the detector analogue to digital converter (ADC) for the high counting rates in the low energy loss part of the spectrum, whereas a pulse counting mode is used for the low counting rates in the high energy loss part of the spectrum, the transition between the two domains being a priori fixed at a given energy loss channel. The important parameters are the number of channels used for recording a spectrum, the channel energy increment, the dwell time per channel and the counting rate. When one is interested by a specific edge, an acquisition is made over 1000 channels with a 0.2 eV step increment such as shown in figure 4, whose caption lists

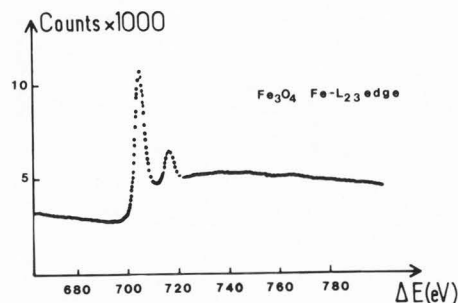


Fig. 4 - Experimental spectrum for studying the Fe L_{23} edge in Fe_3O_4 . The recording conditions are the following: $\alpha_0 = 15$ mrad; $d = 4$ nm; $I_0 = 6.10^{-10}$ A; $\delta = 3.375 \cdot 10^{-10}$ cm²; $t = 600$ ms/channel.

the employed experimental conditions.

The results can then be processed for display in a useful way. A simple program strips the background by fitting to a model law generally chosen as $A(\Delta E)^{-R}$, following Egerton (1975). The determination of the A and R parameters is made by a least-square fit method over typically one hundred channels before the edge, following a Curfit program written by Trebbia (see Colliex et al., 1981). All results in the following paragraphs are shown after such a background stripping, to reveal the fine structures in a way similar to the illustrative diagram of figure 2.

One major feature in EELS is the occurrence of plural scattering which becomes important when the sample thickness approaches the total mean free path for inelastic scattering (typically 50 to 100 nm for 100 kV primary electrons). It introduces satellite edges in core edge spectra, which are due to the possibility of core and plasmon excitations by a single incident electron. These structures are shifted from the single scattering core edge by an energy equal to the plasmon energy and can be confused with real near edge structures, such as shown in fig. 6. for boron and nitrogen K-edges in specimens of increasing thickness. Programs for removing plural scattering events from core edge spectra have been developed by several authors, e.g. Johnson and Spence (1974) or Swyt and Leapman (1982). They can be classified either as Fourier-log or Fourier-ratio method, the first one being more advantageous at the price of more computing time because it also removes plural scattering from the background (Egerton, private communication, 1984). These methods have not been used in the present study but should be implemented for further developments, when one wants to take into account Near Edge Structures lying more than one plasmon energy above the edge. However, they are of less use when one is more concerned by the changes in edge shape, closer than the first plasmon loss to the edge.

A final comment should be made concerning the absolute energy values in spectra reported here. Where possible, features have been calibrated against well-known edges or peaks such as the π^{*} peak on the contamination carbon K-edge. Our impression is that absolute energy values are reliable to ≈ 1 eV.

Theoretical considerations

Without introducing a detailed mathematical treatment, it is useful to provide some general guidelines for the interpretation of the observed spectra. Since the first experiments on absorption spectra, it was postulated that the intensity was determined by the product of a probability of transition $P(\Delta E)$ with a density of states (DOS) for the unoccupied final states $N_C(\Delta E)$, such as :

$$I(\Delta E) \propto P(\Delta E) \cdot N_C(\Delta E) \quad (2)$$

The first term $P(\Delta E)$ is governed by a matrix element between the initial and final states involved in the transition. Let us consider first a one-electron transition in which one core-electron is excited to an unfilled state : the initial state is described by $|i\rangle = |k_0, 0\rangle$ for an incident free electron of wave vector k_0 and a core electron wave function $|0\rangle = |\psi_{n, \ell}(\vec{r})\rangle$ and the final state by $|f\rangle = |k, n\rangle$ with a scattered free electron of wave vector $k = k_0 - q$ and an excited electron wave function $|n\rangle = |\psi_{\varepsilon, \ell'}(\vec{r})\rangle$. In this latter case, one refers to a vacuum state wave function of energy ε and angular momentum ℓ' . The transition matrix element

$$P(\Delta E) \propto |\langle i | H_i | f \rangle|^2 \quad (3)$$

where H_i is the Coulomb interaction Hamiltonian, is governed by the dipolar term :

$$|\langle \psi_{n, \ell}(\vec{r}) | \vec{q} \cdot \vec{r} | \psi_{\varepsilon, \ell'}(\vec{r}) \rangle|^2 \quad (4)$$

in the small angle limit because one approximates $e^{i\vec{q} \cdot \vec{r}} = 1 + i\vec{q} \cdot \vec{r}$. As a consequence, one obtains the well known selection rules $\ell' = \ell \pm 1$, so that one deals in an equivalent photoabsorption or a core-loss EELS measurement with a projection of the unoccupied density of states on a given type of momentum symmetry. Some success has been obtained with this first simplified description, especially in the case of metals (see for instance Colliex and Jouffrey (1972), or more recently Grunes (1983): the near edge structure reflects the partial density of states obtained from a band structure calculation, provided the matrix element factor is slowly varying with energy in this region.

In the case of compounds, this method is insufficient because it neglects an important effect, which can be described as a "local density of states" such as introduced 30 years ago by Friedel (1954). A very complete review of the present state of representation of the electronic structure from the point of view of the local atomic environment can be found in Heine (1980) ; he defines

$n(E, \vec{r}) = n(E) \cdot |\psi_E(\vec{r})|^2$ in which the total density of states $n(E)$ is modulated by $|\psi|^2$ for a "typical" state of energy E . Roughly speaking, a core edge spectroscopy measurement provides a picture of $n(E, \vec{r})$ on an atom, decomposed according to different angular momenta ℓ with the projection operators introduced by dipolar rules. There is a double projection on the unoccupied density of states, one in space on the site of the core hole and one in symmetry.

Following Hayes and Boyce (1982) and Noguera (1981), this can be expressed on a more mathematical basis by introducing the Green function for the final state. One writes the intensity of the core loss excitation on the initial orbital $|\psi_0(\vec{r})\rangle$ as :

$$W_{on}(\Delta E) \propto \langle \psi_0(\vec{r}) | e^{i\vec{q} \cdot \vec{r}} | \text{Im} G(\vec{r}, \vec{r}', \Delta E) | e^{i\vec{q} \cdot \vec{r}} | \psi_0(\vec{r}) \rangle \quad (5)$$

where the G operator of the excited electron can be developed in terms of scattering events as :

$$G = G_0 + G_0 V G_0 + \dots \quad (6)$$

The zero order term G_0 neglects all scattering on the surrounding atoms⁰; it represents the atomic term, because $W_{on}(\Delta E)$ is then equal to :

$$\sum_n |\langle \psi_0(\vec{r}) | e^{i\vec{q} \cdot \vec{r}} | \psi_n(\vec{r}) \rangle|^2 \quad (7)$$

using the definition of the Green function:

$$\frac{1}{\pi} \text{Im} G(\vec{r}, \vec{r}', \Delta E) = \sum_n |\psi_n(\vec{r})\rangle \langle \psi_n(\vec{r}') | \delta[\Delta E - \frac{\hbar^2}{2m}(k_0^2 - k_n^2)] \langle \psi_n(\vec{r}) | \quad (8)$$

When one uses the expansion of the above scattering series to first order, the expression corresponds to single scattering and can be rewritten as :

$$\sum_n |\langle \psi_0(\vec{r}) | e^{i\vec{q} \cdot \vec{r}} | \psi_n(\vec{r}) \rangle|^2 (1 + \chi(\vec{q})) \quad (9)$$

where one recognizes the modulation factor $\chi(\vec{q})$, introduced in EXAFS theory. It actually contains information on the nearest neighbours in this single scattering approach and detailed calculations of $\chi(\vec{q})$ are found in Lee and Pendry (1975). The natural development consists of introducing higher order terms which correspond to multiple scattering from the environmental atoms (see Fig. 5). This is the method followed by Durham et al. (1981) and (1982) for the calculation of X-ray absorption near-edge structure (XANES). We can check that it is formally equivalent to a local density of states because one can rewrite :

$$n(E, \vec{r}) = \frac{1}{\pi} \text{Im} G(\vec{r}, \vec{r}, E) \quad (10)$$

as shown by Heine (1980). In practice, the multiple scattering calculation is done in real space by considering a cluster of atoms surrounding the excited atom. This approach can accommodate such requirements as the use of an excited atom potential for the absorbing atom, which cannot be done very conveniently in a band structure calculation. Within the framework of the tight-binding approximation an expansion of the solid state wavefunctions as a linear combination of atomic orbitals greatly reduces the required computing time for finite clusters. Disko et al. (1984) have recently performed such a simplified calculation of the p-DOS localized at the excited atom for both Be and C in a Be₂C structure.

In the above description, the remaining electrons of the solid have been assumed to be unperturbed in their original states during the one-

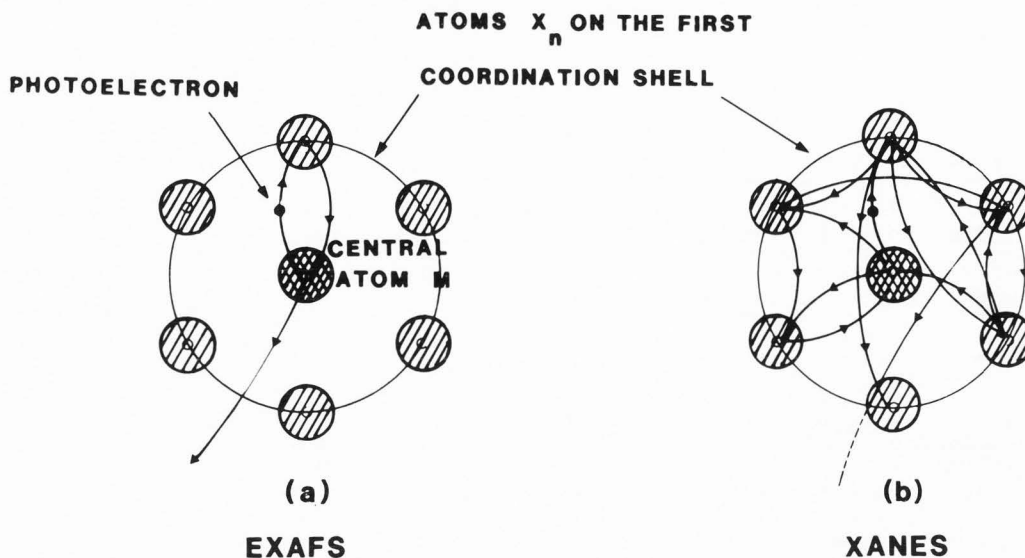


Fig. 5. Schematic view of the multiple scattering processes on neighbouring atoms for the calculation of XANES on the excited atom. (Courtesy of Bianconi, 1981).

electron core excitation. What is the importance of multielectron effects in XANES, such as the relaxation of the valence electrons to screen the core hole or the induced core-hole excited electron interaction? In the case of a metallic alloy, one can expect that the free conduction electron gas efficiently screens the hole created in the core level. The importance of many-body correlations has been the subject of several papers in the late sixties-early seventies (see for instance Mahan, 1974 and Dow, 1974) concerning the shaping of K or L₂₃ edges. Altogether, the energy width of such effects was predicted to be smaller than typically 0.3 eV and therefore inaccessible in most EELS experiments.

The situation is however very different for insulators with band gaps of a few eV between the filled valence and unfilled conduction bands. In this case, the core-hole is poorly screened by the valence electrons which are involved in localized bonds, so that there generally remains a strong coulomb interaction between the core-hole and the excited electron leading to the likely formation of core-excited states. As pointed out by Grunes (1982) the symmetry projected final states of the transitions are not those of the unperturbed initial solid. One must consider the influence of a partially screened hole and it is not expected that such a final DOS will be equivalent for excitations on different atoms in the same solid. Even for atomic spectra, the influence of many electron effects cannot be ruled out, various intrashell and inter-shell correlations being involved in the exact description of delayed atomic spectra of type b and d described above (Amusia, 1974 and Wendin, 1974). Further examples will be given in the next section.

In summary, a hierarchy of contributions can be referred to when attempting to understand features in the near edge structure :

- . atomic effects, with or without multielectron correlations ;
- . environmental effects, determined by the local density of states on the excited electron site.

These are governed mainly by spatial site and angular momentum symmetries and can (or cannot) be accompanied by multielectron rearrangements. A description in terms of molecular orbitals naturally constitutes a first step for describing this environmental contribution because the nearest neighbour bonding largely defines the symmetry of the unoccupied wave functions on the core-hole site.

Results and discussion

General comments.

The number of accessible edges in EELS is very large as shown by the great number of spectra displayed in libraries such as the one edited by Ahn and Krivanek (1982). It becomes enormous as soon as one is concerned about fine structure changes in different chemical environments and crystallographic structures (for instance, there are twelve forms of silica structures !!). The present work remaining limited, it contains a subjective choice of compounds. We concentrate on oxides, because apart from their natural abundance, the oxygen K edge cannot be easily studied with synchrotron techniques. We have added some other edges for low Z elements and have decided to classify them in the following section, as a function of their angular momentum symmetry, since the dipolar approximation constitutes a major rule for interpreting lineshapes.

In all cases, an effort has been made to record spectra from well defined specimen areas and crystallographic structures, checked by standard imaging and diffraction techniques.

Boron K-edge. (Fig. 6)

For all K edges studied here, the general atomic profile is hydrogenic consisting of a saw-tooth shape with a steep edge followed by a monotonically decreasing tail.

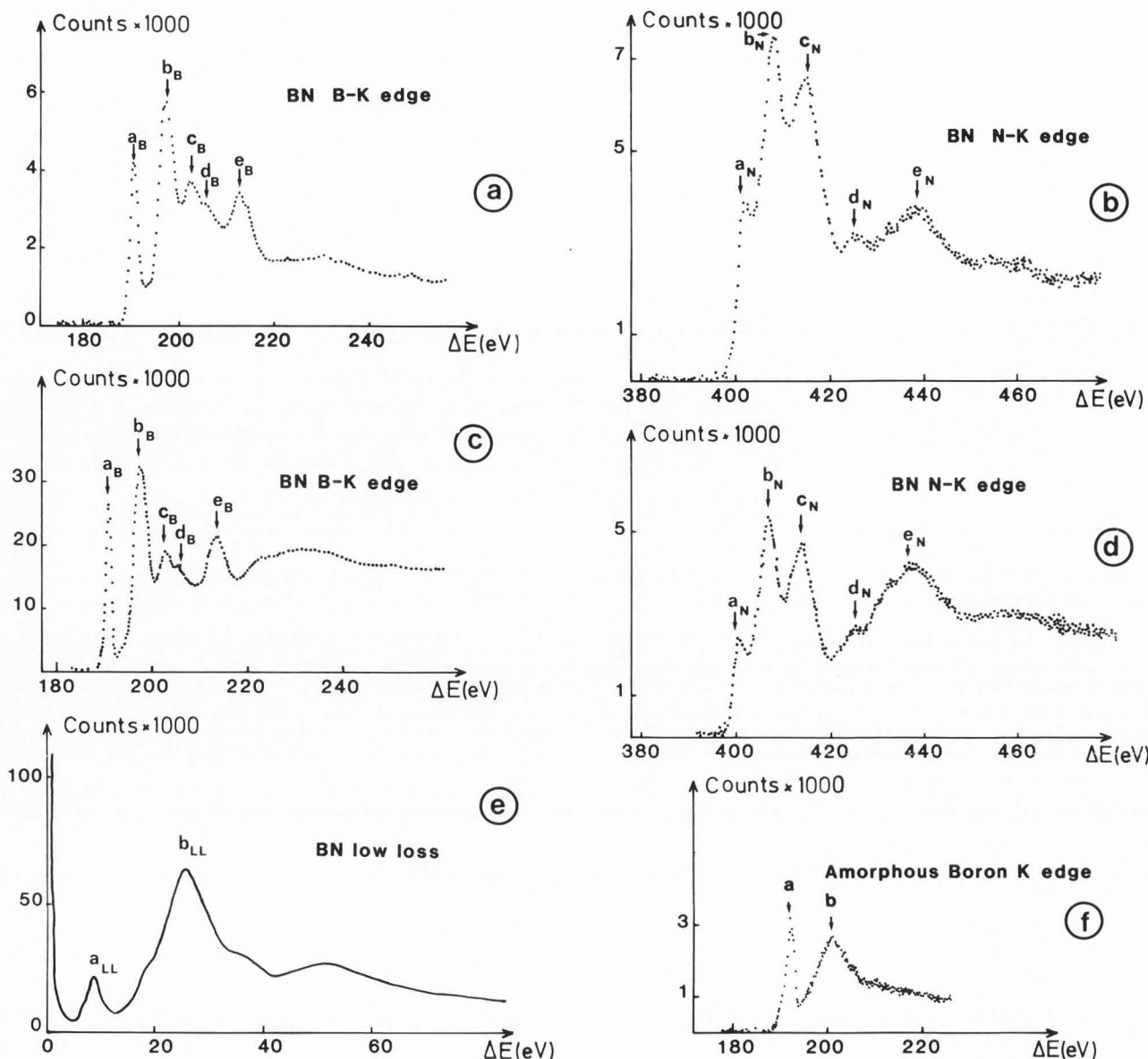


Fig. 6. (a,c) Near Edge Fine Structure of B-K edge in a hexagonal Boron-Nitride.
 (b,d) Near Edge Fine Structure of N-K edge in a hexagonal Boron-Nitride.
 (e) Low loss spectrum of hexagonal Boron-Nitride.
 (f) B-K edge in an amorphous Boron.

Boron-Nitride (BN).

The specimen consists of thin flakes of hexagonal graphitic BN deposited on a holey carbon film. One chooses protruding areas to get rid of the carbon K edge contribution. Thickness ranges from typically 10 to 50 nm and the influence of multiple scattering is illustrated by comparison of the B and N-K edges for thin and thicker areas (Figs. 6a, 6b, 6c and 6d): the relative intensity of peaks marked d and e with respect to peaks a, b and c closer to the edge clearly depends on specimen thickness. For interpretation, a low loss spectrum is shown in Fig. 6e which exhibits two main features a_{LL} and b_{LL} . It seems reasonable to assume that in the BN-nitrogen K edge, peaks d_N and e_N correspond to multiple scat-

tering events involving the a_{LL} and b_{LL} low loss features. Table 1 summarizes the energy positions of all peaks appearing in Figure 6.

When one considers the relative energy separation of the main three peaks a, b and c in both boron and nitrogen K edges, it is clear that they coincide to within 1 eV although their relative intensity varies. This observation may be taken as evidence that both transitions, originating from similar 1s orbitals localized either on boron or on nitrogen atoms, go to the same $\ell = 1$ type of final state. Moreover both sites have the same co-ordinate geometry comprised of atoms of the other species, in the graphitic structure ($a = 2.51 \text{ \AA}$, $c = 6.66 \text{ \AA}$).

Our experimental results provide high resolution spectra which confirm previous ones (Colliex, 1984a, Hosoi et al., 1982, Leapman et al., 1983, Stephens and Brown, 1981). The interpretation of these data has been formulated from the beginning in terms of unperturbed DOS of unfilled conduction states, following several band calculations such

TABLE 1*

Energy position of all peaks appearing in Fig. 6.

	a eV	b eV	c eV	d eV	e eV
BN-Boron K edge	190.90 ± 1.0	197.70 ± 1.0	203.20 ± 1.0	206.30 ± 1.0	214.10 ± 1.0
BN-Nitro- gen K edge	400.30 ± 1.0	406.70 ± 1.0	413.70 ± 1.0	425.40 ± 1.0	438.10 ± 1.0
BN-Low Loss Spectrum	8.70 ± 1.0	26.30 ± 1.0			
Amorphous Boron K edge	192 ± 1.0	200.6 ± 1.0			

* Note that although the full width half maximum resolution of the spectrometer is of the order of 1 eV, the maximum in a spectral peak can be located very much more accurately.

as Nakhmanson and Smirnov (1972). The peak labeled a is associated with a π^{**} type final orbital (in the direction perpendicular to the hexagonal lattice planes) while peaks b and c refer to σ^{**} type final orbitals in the hexagonal plane. This model is supported by the detailed work of Leapman et al. (1983) who have investigated the orientation dependence of these core edges. If a configuration of crystal and collector aperture is chosen which favours momentum transfer parallel to the π bond, the corresponding π^{**} peak is more intense and, for momentum transfer in the hexagonal plane, it vanishes with respect to the σ^{**} peaks. In our experimental conditions, the large acceptance angle of the spectrometer mixes both contributions and the recorded spectrum gives a rather good representation of the total DOS of unoccupied states, including both π and σ type molecular orbitals. It is not yet clear whether the exact absolute position and intensity distribution in these three peaks has to be attributed to core-exciton features or to local density of states effects. Finally we note that Hosoi et al. (1982) have compared these characteristic B and N-K edges in several types of crystalline structures, including hexagonal type as above, cubic type and wurtzite type. There again a rough agreement with DOS-calculations seems to exist.

Amorphous boron.

The last spectrum (Fig. 6f) corresponds to a thin foil, typically a few nm thick of amorphous boron as prepared by Dorignac et al. (1979). The fine structure is much poorer: it only consists of a narrow peak followed by a broader and less intense one at 8 eV higher energy. Similar features will be described below in molecular systems. It seems reasonable to think that since there is no well organized order around any of the excited atoms, one has to assign a fundamental Rydberg final state for peak a followed by transition to the continuum for peak b.

Carbon K-edge. (Fig. 7 to 11)

In solid samples, the carbon K edge is the most frequently studied case. Fig. 7 shows the spectra recorded in the three main types of carbon specimen: amorphous carbon (7a), graphite carbon (7b), diamond carbon (7c) plotted on the same energy scale. There exist strong similarities between Figs.

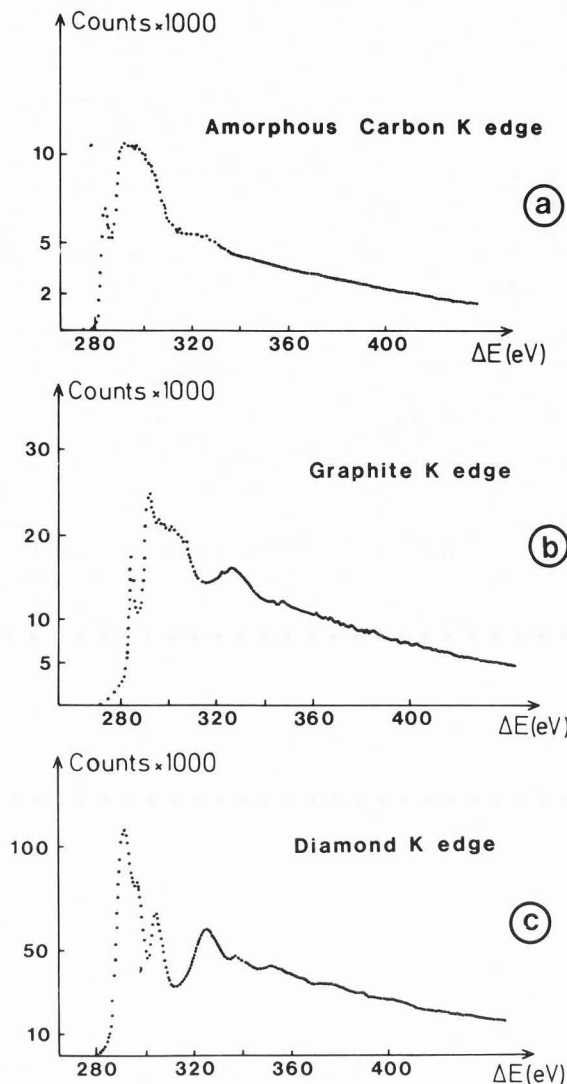


Fig. 7 - Near Edge Fine structure of C-K edge in: (a) amorphous carbon; (b) graphite carbon; (c) diamond.

7a and 7b with the presence of a narrow peak typically 1.5 eV wide at the edge, followed by a maximum lying 6 or 7 eV above. In the graphite case the structure ranging from about 6 to 40 eV above the edge displays clearer modulations. Following earlier work, one can attribute the origin of the peak at the edge to a π^{**} molecular orbital and those in the subsequent band to σ^{**} unoccupied states, as has been confirmed by the orientation dependence experiments of Leapman et al. (1983). The general agreement with unperturbed DOS curves must not prevent one from pointing out the fact that the π^{**} peak lies at an energy typically 2 eV below the predictions of the theory while the agreement is better for the σ^{**} peak. This effect has been more thoroughly considered by Mele and Ritsko (1979) in a study of the 1s-carbon fine structure in intercalated graphite. They have clearly shown that the π^{**} line shape and position differ from a ground state calculation. They have developed a scattering theory formalism similar to the one mentioned

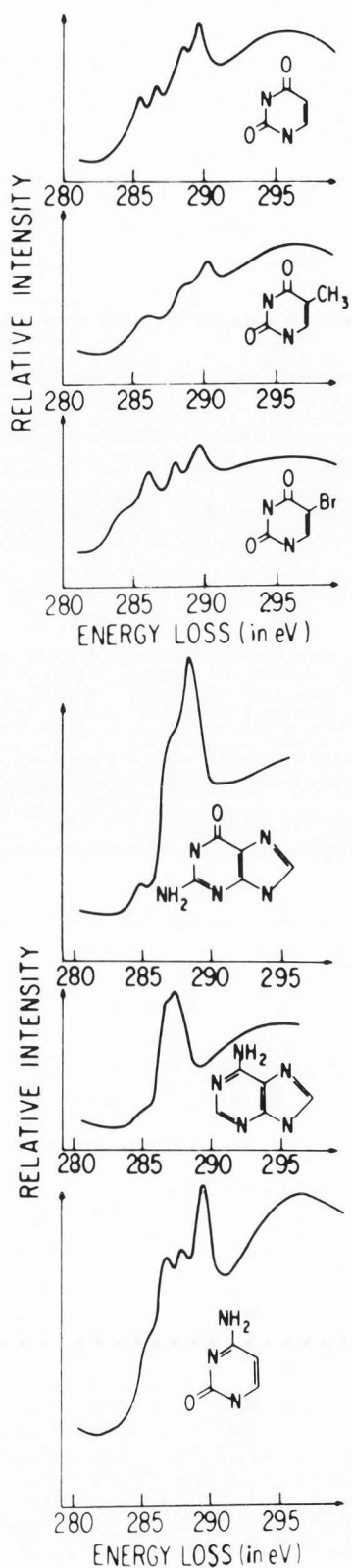


Fig. 8 - Comparison of the threshold of the carbon K-edge in six types of nucleic acid bases (courtesy of Isaacson, 1979).

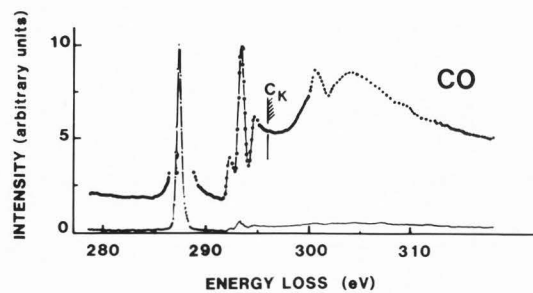


Fig. 9 - Carbon K-shell energy loss spectrum of molecular CO. (courtesy of Hitchcock and Brion, 1980).

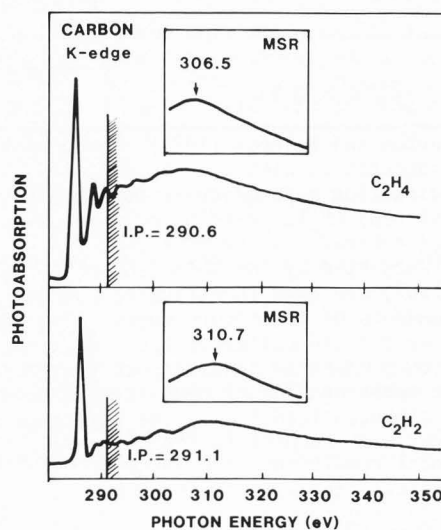


Fig. 10 - K-edge spectra of C_2H_2 and C_2H_4 showing the MSR resonance above $E_0 = I.P.$. The MSR shifts towards higher energy with decreasing interatomic C-C distance. (courtesy of Bianconi, 1981).

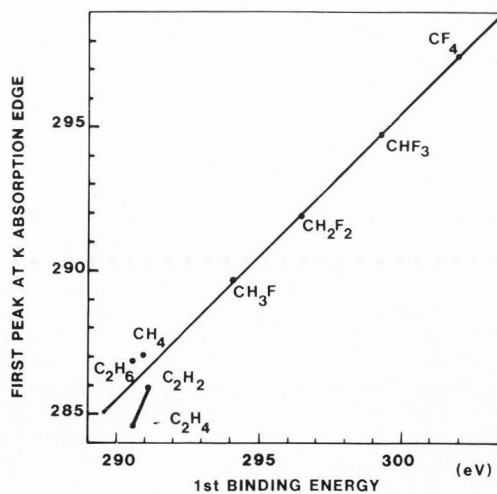


Fig. 11 - Chemical shift of the first excited state at the K-edge of C in several molecules. (courtesy of Bianconi, 1981)

above to predict the density of states in a non-periodic structure with a core-hole on one site. It comes out that the labeled π^{**} peak corresponds more to a core exciton than to the ground state density of the antibonding π bond. We think that these considerations could be extended to explain the narrow and intense π^{**} type peak which is also present in the case of amorphous carbon.

For the diamond case, there are strong differences with the preceding spectra: one notices first a "shift" of edge position of the order of 5 eV, which corresponds more to a disappearance of the π^{**} peak. The additional structures above 290 eV have been interpreted qualitatively in terms of the unperturbed DOS by Egerton and Whelan (1974). The difference between the graphite and diamond fine structures is understandable in terms of the difference in orbitals hybridation (sp^2 versus sp^3).

In the above spectra from solid carbon specimens, there is no need to distinguish different sites because they are all equivalent. The problem becomes even more difficult in specimens involving molecular bonds with atoms of different nature. This situation is illustrated by some examples. Fig. 8, from Isaacson (1979), clearly shows the difference in edge shapes for carbon atoms involved in different molecular environments in nucleic acid bases. Fig. 9 concerns the K-edge of carbon in molecular CO from Hitchcock and Brion (1980) and, for illustration, Fig. 10 is an example of a photoabsorption spectrum in the same energy range for C_2H_2 and C_2H_4 molecules from Pittel et al. (1979). In such spectra, two regions can be easily defined because in molecules the energy E_0 of the threshold of transition to continuum states in the vacuum can be unambiguously measured independently by ESCA (Electron Spectroscopy for Chemical Analysis) - E_0 is the energy of the core ionization potential. Therefore, one separates the region of discrete transitions below E_0 , which is characterized by an intense narrow peak, and the continuum transition above E_0 . In this second domain, Bianconi (1981) has shown how the excited electron with low kinetic energy is strongly scattered by neighbouring atoms and is therefore in the multiple scattering regime. These multiple scattering resonances labeled MSR in Fig. 10 are governed in number and intensity by the symmetry of the molecules - the example shown being typical for a linear molecule.

In contrast, the fine structure below the ionisation edge, that is the main peak in Figures 9 and 10, is due to transitions to unoccupied valence orbitals. Bianconi (1981) has derived a correlation between the chemical shift in E_0 defined above, and the first excited state in molecules with similar geometry, as shown in Fig. 11. This graph could be used to obtain information on the effective charge of the absorbing atom. These examples show the importance of molecular studies for understanding the origin of edge fine structures. Of course, it is not at present possible to determine the ionization energy from energy loss spectra in the solid state.

Molecular N_2 and O_2 -K edges. (Fig. 12)

Before considering oxygen K-edge shapes in various oxides, it is useful to show spectra of the K-edge

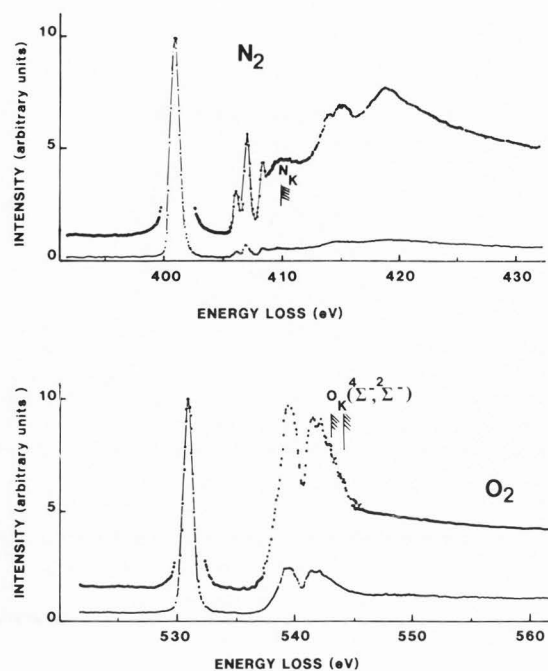


Fig. 12 - K-shell energy loss spectrum of N_2 .
K-shell energy loss spectrum of O_2 .
(courtesy of Hitchcock and Brion, 1980)

for nitrogen and oxygen in N_2 and O_2 gases as recorded by Hitchcock and Brion (1980) (Fig. 12). Both spectra show similar features, namely an intense discrete line followed by structures of weaker intensities clearly revealed upon vertical scale expansion. Also marked on the figures are the location of the nitrogen and oxygen 1s ionization thresholds. The interpretation of these spectra involves a transition to a final $2p\pi_g(\pi^{**})$ orbital for the intense line which is the main contribution of oscillator strength for transitions to unoccupied discrete states, together with some of the fine structure before the ionization edge assigned to transitions 3s, 3p and 4s molecular orbitals. Concerning transitions to the continuum, there can exist resonance effects due to the molecular centrifugal barrier acting on the higher ℓ components of the final states, as pointed out by Bianconi (1981). *Oxygen K-edge in oxides.* (Figs. 14 to 17) The results are gathered in three figures, being devoted respectively to light metal oxides (MgO , Al_2O_3 and SiO_2) in Fig. 14, to transition metal oxides (Sc_2O_3 , TiO_2 and NiO) in Fig. 16 and to rare earth oxides (La_2O_3 , Gd_2O_3 and Yb_2O_3) in Fig. 17. The major specimen characteristics are listed below.

MgO - Small cubes are obtained by burning magnesium foil in the air. The resulting monocrystals were analyzed with (100) axis parallel to the beam. Rock-salt structure with $a = 4.21 \text{ \AA}$. Fig. 13a shows a typical micrograph: EELS analysis is performed on cubes of typical thickness

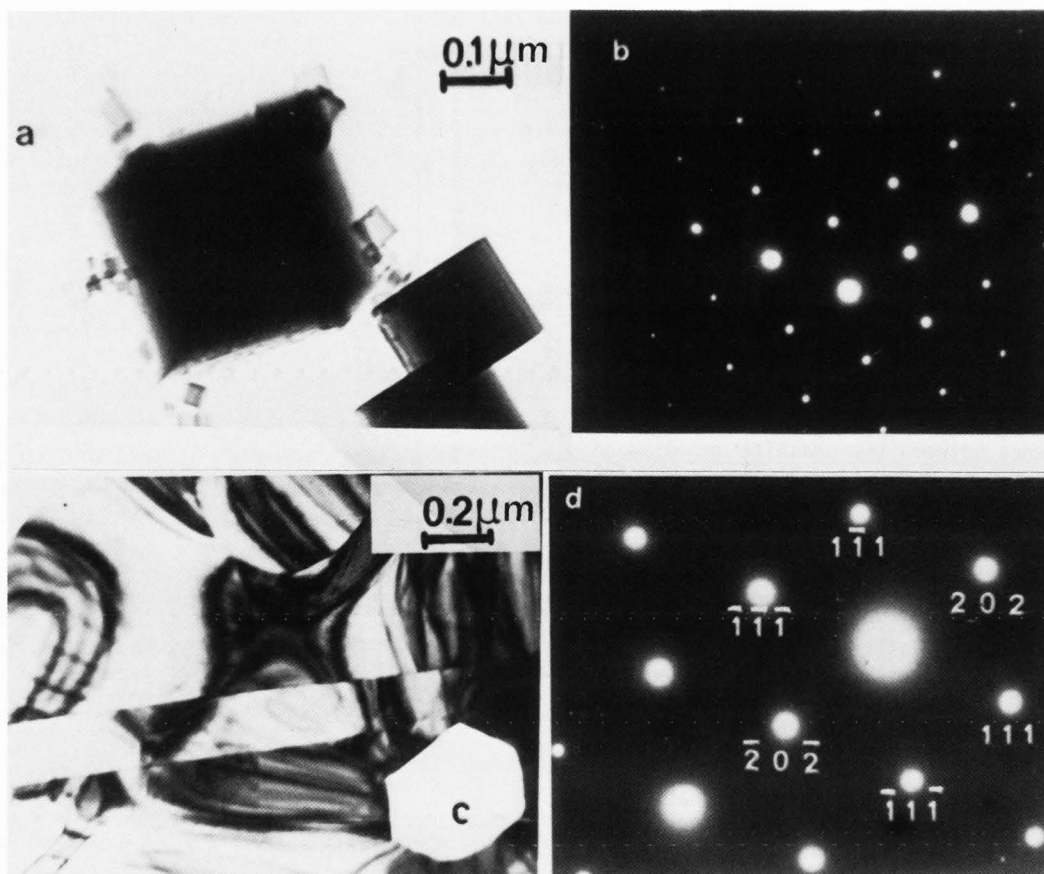


Fig. 13 - (a) Micrograph on the cube of MgO.
 (b) Electron diffraction pattern on NiO.
 (c) Micrograph on Gd₂O₃.
 (d) Electron diffraction pattern on Gd₂O₃.

25 to 50 nm. Both Mg and O atoms have the same octahedral environment.

Al₂O₃ - The specimen is the γ_t alumina support used for studies of Pt clusters catalysts. It is actually a hydrated alumina (Al₂O₃, xH₂O with $0 < x < 0.6$) obtained after thermal treatment of boehmite. The observed structure is tetragonal with a slight distortion ($c/a = 0.98$) compared with the cubic structure, in which case $a = 7.9 \text{ \AA}$ (courtesy of Institut Français du Pétrole).

SiO₂ - The specimen is a monocrystal of α -quartz prepared by ion thinning. The α -quartz is hexagonal built on a fundamental structural unit, the SiO₄ tetrahedron. All silicons are surrounded by four oxygens in the tetrahedral directions, but each oxygen is bonded to only two silicons and the Si-O-Si angle, ϕ , varies from one allotrope to another. As a consequence of beam irradiation one preserves the constant tetrahedral environment for the Si-atom, but introduces quite variable environments for the oxygen atoms.

Sc₂O₃ - See R₂O₃ cubic structure (below).

TiO₂ - Rutile form - monocrystal prepared by ion thinning. It crystallizes in a tetragonal lattice in which the oxygen atoms are arranged in a distorted octahedron around the titanium atom

and three titanium atoms lie in a plane around the oxygen atom (see Grunes et al., 1982, for a complete calculation of crystal and band orbitals for TiO₂).

NiO - It is crystallographically similar to MgO with a rocksalt type structure ($a = 4.18 \text{ \AA}$) in which both Ni and O atoms have the same well defined octahedral environment. The specimen is a monocrystal prepared by ion thinning. Fig. 13b shows a characteristic electron diffraction pattern.

Rare-earth oxides R₂O₃ (including Sc₂O₃).

The specimens are thin evaporated foils of rare-earth metals heated in the electron microscope column under the primary electron flux (see Gasgnier, 1980, for details). Rare-earth oxides (R₂O₃) are polymorphic chemical compounds characterized by three crystallographic structures: A-type (hexagonal), B-type (monoclinic) and C-type (b.c.c.). Each one is described as a succession of slabs of the complex cation [RO]ⁿ⁺ separated by oxygen anion planes (Caro, 1968).¹¹ When heated at high temperature, the A structure is obtained for La, Pr and Nd sesquioxides, the B structure for Sm, Gd and Tb sesquioxides and the C structure for the heavier rare-earth oxides including the scandium oxide (scandium can be considered for many reasons either as a transition metal or a rare-earth metal). Without delving into a detailed

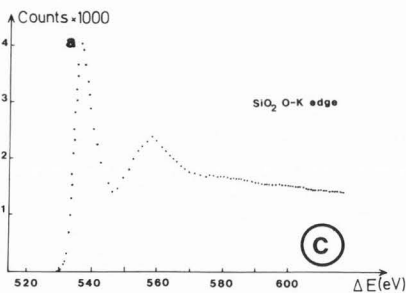
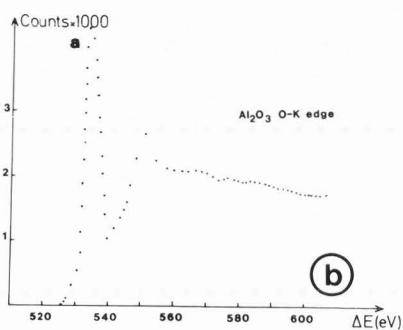
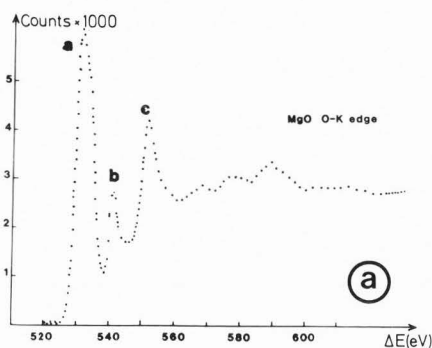


Fig. 14 - Near edge fine structures for the O-K edge in (a) MgO ; (b) Al_2O_3 ; (c) SiO_2 .

description of the corresponding structures, let us point out that in all cases the oxygen atoms are approximately tetrahedrally surrounded by four metal atoms, the difference between these three crystal structures occurring in the second nearest neighbour and the metallic site environments. Figure 13c shows a characteristic image of a $B Gd_2O_3$ large crystal with typical twins and holes contours - in this monoclinic structure the angles between the hole edges are not exactly 120° as in a characteristic A-type oxide. Figure 13d presents the corresponding diffraction pattern with a pseudo-hexagonal symmetry.

For the three light metal element oxides in Fig. 14, the edge consists of a major single peak (a) at the edge, the position of which shifts

gradually towards higher energy losses from MgO to SiO_2 . All spectra display also a weaker and broader peak at energies lying between 15 eV and 25 eV above the first one, for which an explanation in terms of a plasmon satellite cannot be ruled out. The MgO K edge shows moreover an intermediate peak (b) at 542 eV. To interpret these features, one can note that in both Al_2O_3 and SiO_2 the general environment of the oxygen atoms is poorly defined. Concerning the more well defined MgO case, the major peak at the edge (5 eV wide) does not seem to be split for an octahedral environment.

The discussion can be developed by comparing this result with the associated Mg K-edge in MgO (Fig. 15). Both edges refer to the same $l = 1$

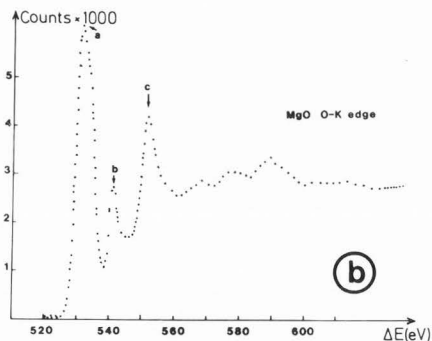
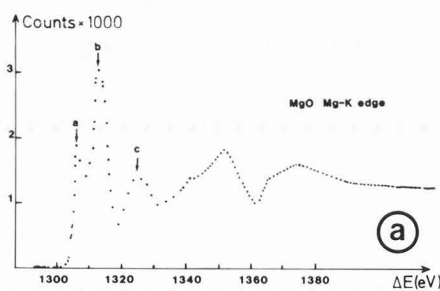


Fig. 15 - Near Edge fine structures of (a) Mg-K in MgO ; (b) O-K in MgO.

symmetry final state and to the same octahedral site symmetry. The present result seems to be in contradiction with the data shown by Taftø and Zhu (1982), in which a prominent 8-10 eV broad quasi-gaussian peak at threshold is seen on K-edges of Mg and Al octahedrally coordinated by oxygen atoms. It is observed that the splitting of the first three peaks are rather similar in both the Mg and O K-edges (Table 2).

Similarly to the BN case which displays the same general trends, the major difference lies in the relative intensity between these three features. One can postulate that the spectral weight is such that the states at the bottom of the band have an enhanced weight on the oxygen atoms and a reduced one on the magnesium atoms. An unperturbed DOS

TABLE 2

Energy position of all peaks appearing in Fig. 14.

MgO	a (eV)	b (eV)	c (eV)	b-a (eV)	c-a (eV)
O-K edge	532.2 ± 1.0	540.8 ± 1.0	552.0 ± 1.0	8.6 ± 0.2	19.8 ± 0.2
Mg-K edge	1305.5 ± 1.0	1312.0 ± 1.0	1324.5 ± 1.0	6.5 ± 0.2	19.0 ± 0.2

Note the improved accuracy in energy difference measurements with respect to accuracy in absolute energy value.

calculation by Pantelides et al. (1974) actually predicts the existence of three such main contributions in the conduction band, the first one being split into two components separated by about 2 eV. The present experimental study offers no clear evidence as to whether these three observed features in the ELNES are due to structure in the unperturbed DOS or to core excitons. In Figure 16, we show three examples of oxygen K near-edge fine structures for Sc_2O_3 , TiO_2 and NiO ; transition metal oxides (not including Sc_2O_3) have been the subject of a very extensive work by Grunes (1982) the part of which concerning the oxygen K edge was published in Grunes et al. (1982) accompanied by original DOS calculations for TiO_2 and NiO . Our discussion will therefore be very limited because everything which can be said in the present state of knowledge and interpretation is expressed in these references. One can notice the close resemblance between our NiO -O K edge and theirs for the position and shape of the first three maxima, our curve containing further structures at higher energy losses. Our TiO_2 -O K edge also shows the splitting of the first two peaks, as does our original work on Sc_2O_3 . Such a splitting seems to be common to the first peak in the oxygen K edge in a tetrahedral environment.

The above hypothesis is confirmed by examination of the oxygen K-edge fine structures in R_2O_3 specimens. Whatever the detailed crystal structure, they seem to be characterized by a main band type profile of about 7 to 8 eV wide, generally split in two peaks. This splitting is very clear for the C-structure, weaker for the A and B-structures (in A, it is generally asymmetric with the second peak more intense than the first one, and in B it is so weak that in some cases it could be confused with a rounded profile, as in a preliminary report (Brown et al., 1984). This general behaviour might be considered, in the absence of more adequate theoretical description, as a fingerprint of the tetrahedral environment for oxygen atoms. L_{23} edges in MgO , Al_2O_3 and SiO_2 . (Fig. 18)

The general behaviour of the L_{23} edges is governed by the atomic-like distribution of the oscillator strengths of $2p \rightarrow nd$ type excitations, because the transition strength to ns-type final states is much lower. Hence L_{23} excitations probe the vacant d-symmetry orbitals. For Mg, Al and Si oxides, these orbitals lie rather high in energy above the edge (typically 15 to 25 eV) giving rise to a delayed maximum as noticed in the early works of

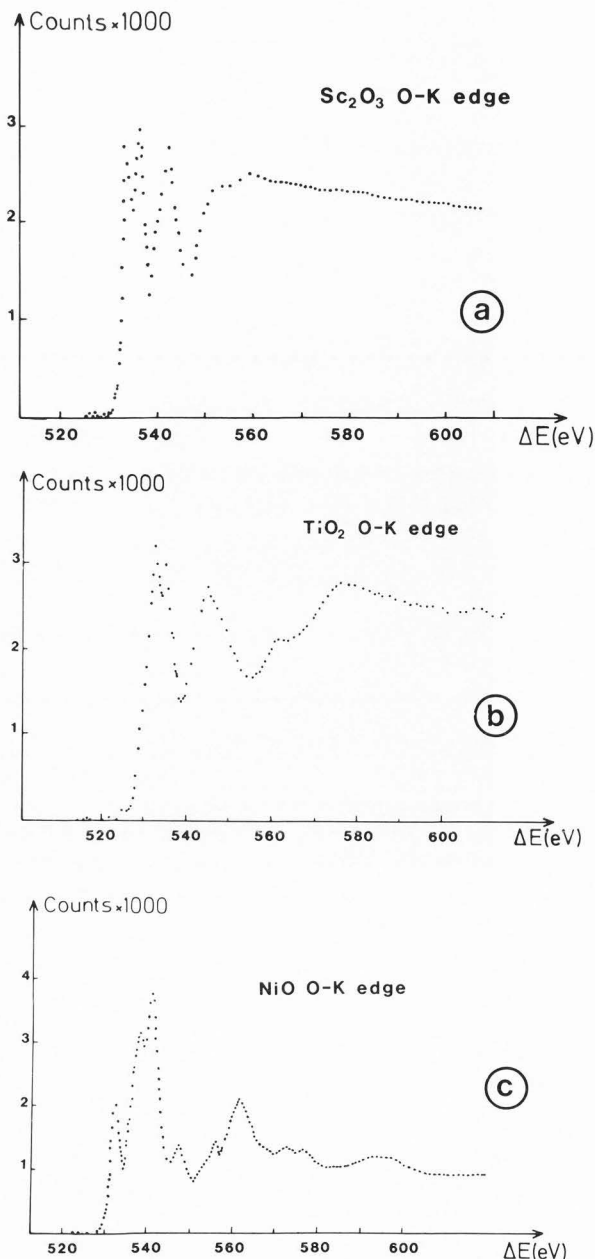


Fig. 16 - Near edge fine structures for the O-K edge in (a) Sc_2O_3 ; (b) TiO_2 ; (c) NiO .

Swanson and Powell (1968) and Colliex and Jouffrey (1972). When one proceeds to transition metal oxides these d-type orbitals move through the Fermi level so that the general shape is very different, appearing as a typical "white line" edge.

In contrast to the O-K edges, the L_{23} edge fine structures are very intense and visible in all cases. This is a consequence of the fact that the local environment of the metallic ion is always well defined. One notices several important effects. The first one is a clear "chemical shift" that is a displacement of the position of the first rise with respect to the pure Mg, Al or Si case. We measure shifts of 3 eV for SiO and 6 eV for SiO_2 by comparison with the L_{23} edge threshold in pure Si at 99.5 eV.

Near edge fine structures on EELS core loss edges

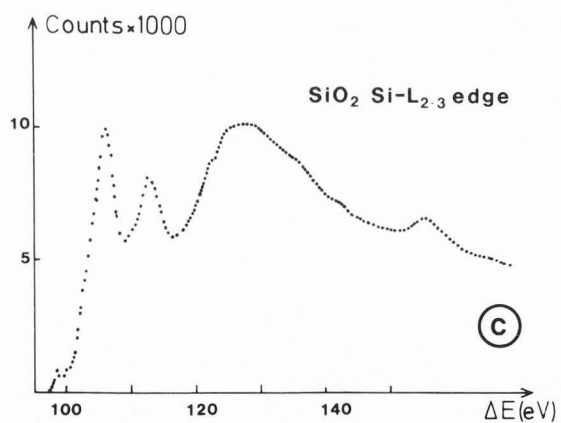
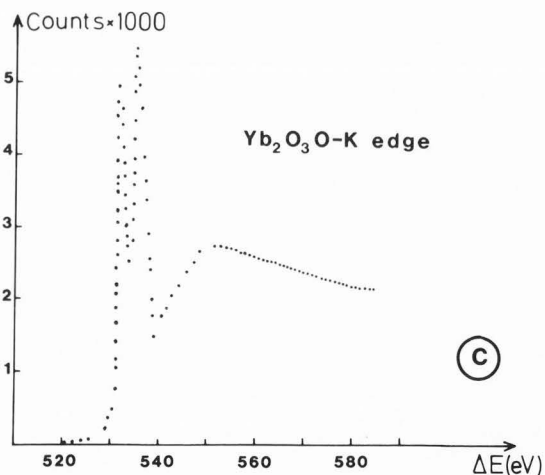
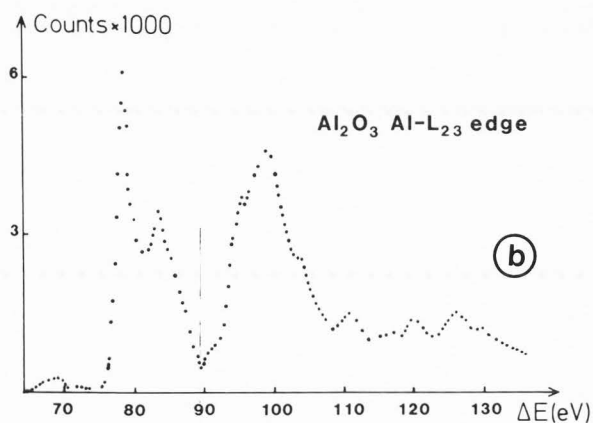
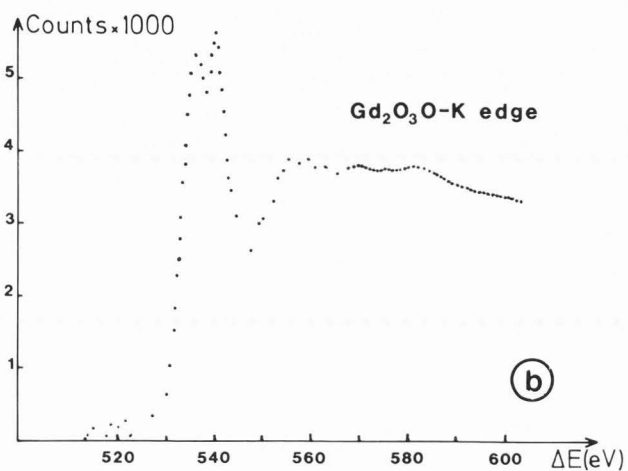
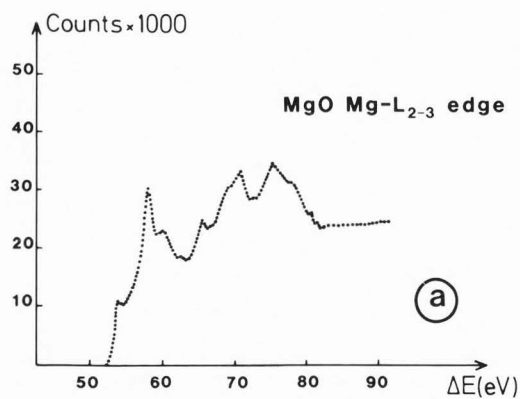
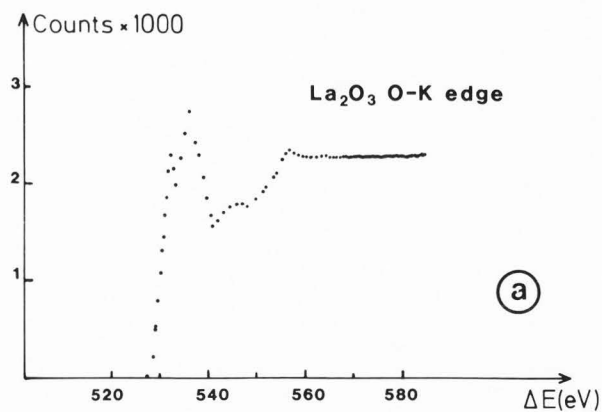


Fig. 18 - The L₂₃ edges in (a) MgO ; (b) Al₂O₃ ; (c) SiO₂.

Fig. 17 - Near Edge fine structures for the O-K edge in (a) La₂O₃ ; (b) Gd₂O₃ ; (c) Yb₂O₃.

An interpretation had been provided by Ritsko et al. (1974) for the general extended modulations between 20 and 80 eV above the edge in terms of EXAFS structures ; it does not predict anything for the structures near threshold. One must then

refer to a XANES type interpretation. Our measured Si L_{23} edge in SiO_2 (Fig. 18c) bears a close resemblance to the absorption curve of Bianconi (1979) for bulk SiO_2 . The near-edge structure is very similar to the XANES of SiF_4 gas, that is a typical example of solid state spectra retaining the main features of gas spectra. This observation confirms our previous hypothesis that the L_{23} XANES (or ELNES) of SiO_2 are mainly due to the microscopic structural tetrahedral unit SiO_4 . Our Al_2O_3 spectrum (Fig. 18b) also bears a close similarity to the synchrotron curve for crystalline Al_2O_3 shown by Balzarotti et al. (1974). In these compounds again, the ELNES are defined by multiple scattering inside the first coordination shell. Such "molecular type" effects could be used to determine the coordination geometry. Altogether these examples, including the well defined MgO situation, constitute valuable experimental data for future investigations to evaluate the role of the projected DOS of the unperturbed solid (as yet uncalculated) in determining the measured spectrum.

L_{23} edges in transition metal oxides. (Fig. 19)

In the 3d transition metal oxides, the metallic 3d orbitals combine with the oxygen 2p orbitals to make up the valence and conduction bands. There exists therefore a high density of unoccupied d states just above the Fermi level, and, as a consequence, an intense probability of transition for 2p-core levels. It is clearly shown in the spectra of Fig. 19, for which most of the intensity is concentrated into the first lines L_3 and L_2 separated by the spin orbit splitting of the initial state, $2p_{3/2}$ and $2p_{1/2}$ respectively.

Apart from our curve for Sc_2O_3 , which is original, the results for TiO_2 and NiO are in good agreement with the data obtained by Grunes (1982) and published in Leapman et al. (1982). The major effect is a superposition of a crystal field effect on the metallic ion sites which splits both the L_3 and L_2 lines into another pair of lines separated by 1.6 eV in Sc_2O_3 and 2.5 eV in TiO_2 . This splitting does not happen for the NiO case. A rather complete discussion of its origin can be found in Leapman et al. (1982) and Grunes (1982). The cluster molecular orbital approach due to Fischer (1971) shows how the octahedral coordination of Ti atoms with oxygen splits the degenerate unoccupied 3d state into lower energy $2t_{2g}$ and higher energy $3e_g$ molecular orbitals separated by an observable energy. For transition metals at the beginning of the d series, both molecular orbitals are unoccupied while for the 3d metals at the end of the series only the upper level remains vacant, precluding the existence of a splitting. This simple molecular orbital theory can predict only spectral peak energies but nothing about their shapes and widths. Consequently, a solid state conduction band DOS has been calculated by Wilker and Hoffmann, for which the Ti-projected DOS is shown in Grunes (1983). The two peaks in the unfilled DOS, centered at about 2.8 and 7 eV in the rutile phase, are however more widely separated than in the experimental results.

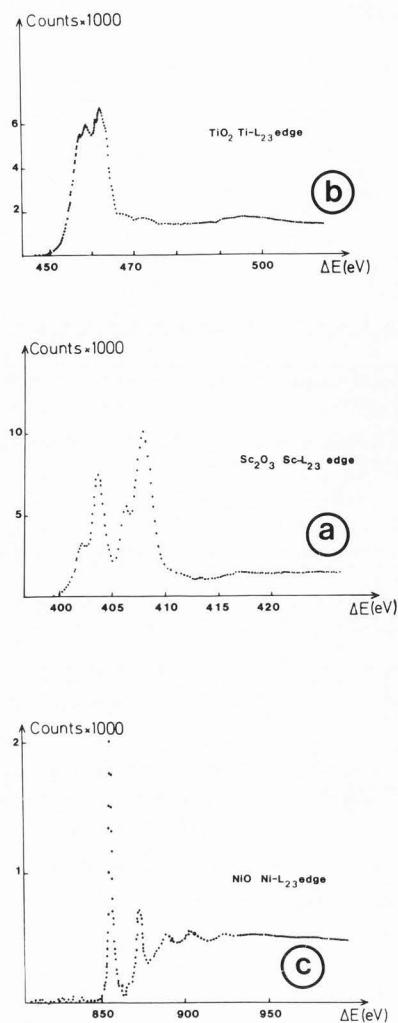


Fig. 19 - The L_{23} edges of transition metals oxides (a) in Sc_2O_3 ; (b) TiO_2 ; (c) NiO .

Another important aspect of the L_{23} edges lies in their absolute energy position when compared to their equivalents in the 3d transition metals. As shown by Leapman et al. (1982), apart from the splitting already mentioned for TiO_2 and the case of Cu and CuO - in which the metal step edge is modified into a peak in CuO due to mixing of Cu d-orbitals and O p-orbitals into the conduction band - the shape of the "white lines" remains rather similar in all other cases. Consequently, one can measure an EELS chemical shift of the L_3 edge, for instance, between oxide and metal in a way very similar to the XPS (X-Ray Photoelectron Spectroscopy) chemical shift. The results are however very different and one does not find in all cases the usual XPS chemical shift towards higher energies for oxides (associated with the fact that the oxide metal 2p level lies deeper than in the pure metal). One must be aware that in XPS the final state for the excited electron lies in the continuum at energies far above the Fermi level,

which is unchanged between metal and oxide. Consequently, the XPS chemical shift only refers to the position of the core 2p level. On the contrary, in EELS as well as in X-ray absorption, the excited 2p electron is in a localized 3d state: the chemical shift is affected both by the position of the 2p core level and by the modifications in unoccupied states close to the Fermi level, such as the creation of a band gap, for instance. The situation is much more complex and Leapman et al. (1982) have discussed several tentative explanations including differences in the relaxation processes of the valence electrons around the core hole.

M₄₅ edges in rare-earth oxides. (Fig. 20)

From $Z = 57$ to $Z = 71$ the rare-earth series is characterized by a progressive filling of the 4f levels from 4f⁰ in La to 4f¹⁴ in Lu. These orbitals are generally described as localized functions lying on each atomic site well within the 5d¹6s² conduction electrons orbitals.

In the present work, we have only considered trivalent rare-earth oxides of type R₂O₃ in which case the R-5d¹6s² wave functions mix with the oxygen 2p wave functions to form the combination of valence and conduction bands.

The M₄₅ edges refer to the excitation of the 3d_{3/2} and 3d_{5/2} R-electrons lying typically between 800 and 1600 eV below the Fermi level. Figure 20 shows five typical examples covering the whole series of lanthanides. They generally appear as "white lines" that is again as a pair of narrow and intense peaks followed by rather constant contributions over which are superposed EXAFS oscillations. Similar data have been published by Krivanek (1982). The two lines can be labeled as M₅ for the excitation of the R-3d_{5/2} electrons and M₄ for the R-3d_{3/2} electrons. As shown in Fig. 21, the energy difference (M₅ - M₄) is a measurement of the spin-orbit splitting of the 3d level. It continuously increases from ≈ 16 eV in La₂O₃ to ≈ 42 eV in Tm₂O₃. Another general behaviour concerns the intensity ratio M₅/M₄ which varies regularly as the number of f electrons increases. At the beginning of the series, the M₅ line is weaker than the M₄, while at the end the M₄ line has nearly completely vanished. In Fig. 21, the intensity ratio is estimated from the peak areas after background subtraction. It can be done with rather good accuracy for the lighter lanthanides, but a great source of error arises for the heavier ones because there is a superposition of the M₄ peak with the low energy loss satellites of the M₅ peak. This constitutes a typical example for which a deconvolution procedure would be useful. As for interpretation, it is clear that the ratio departs from the simple 3/2 ratio which could be predicted from the relative degeneracies of both the 3d_{5/2} and 3d_{3/2} initial level. Instead more complex rules for the probability of transition in intermediate or j-j coupling must be involved. When one considers such a white line in more detail, fine structures are resolved as shown in Fig. 22 for the M₅ edge in Er₂O₃. For comparison, we also show an X-ray absorption spectrum due to Karnatak (private communication, 1984) and the position of

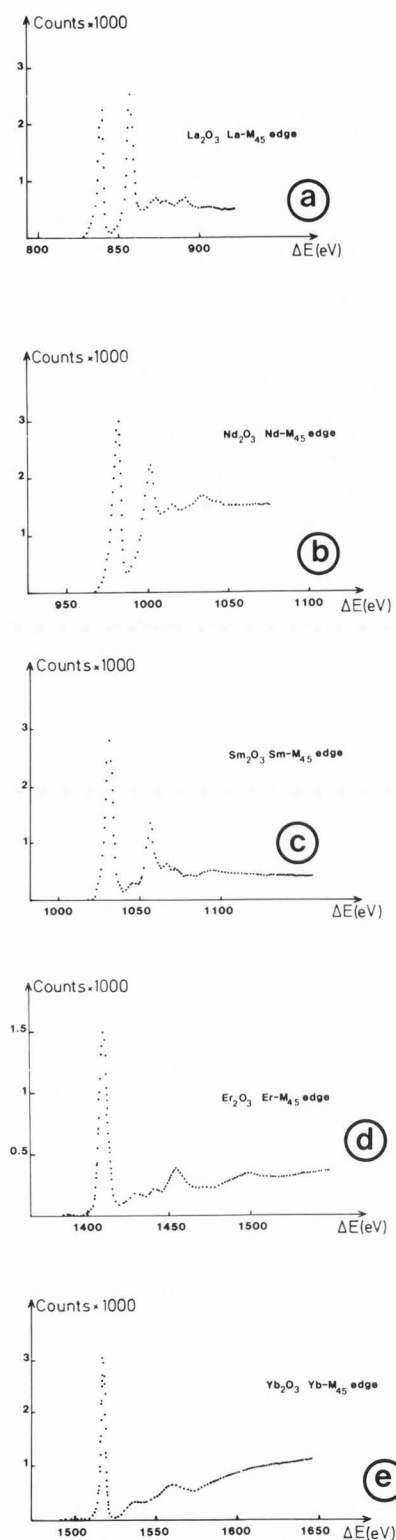


Fig. 20 - The M₄₅ edges in rare-earth oxides :
(a) La₂O₃ ; (b) Nd₂O₃ ; (c) Sm₂O₃ ;
(d) Er₂O₃ ; (e) Yb₂O₃.

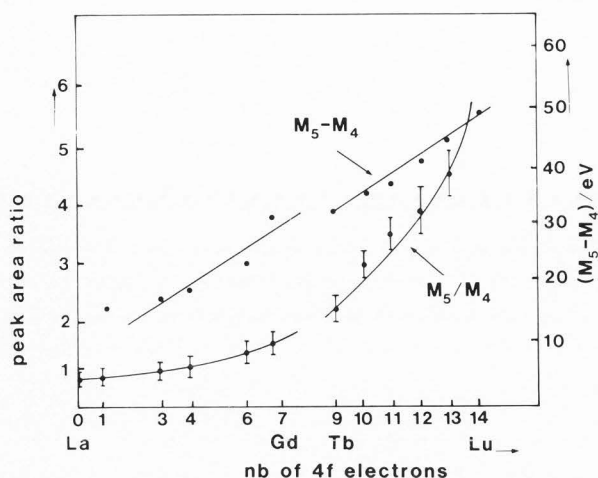


Fig. 21 - Variation in separation and area ratio of the M₅ and M₄ white lines across the series of lanthanide oxides.

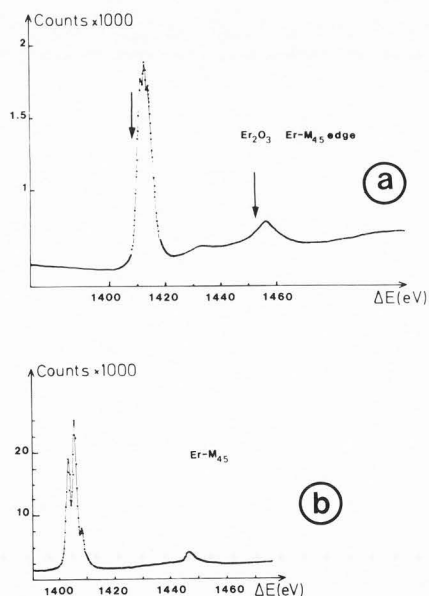
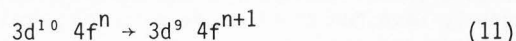


Fig. 22 - (a) M₅ edge in Er₂O₃ obtained by EELS. (b) M₅ edge extracted from X-ray absorption measurements (Karnatak, private communication).

the M₅ line as extracted from photoelectron spectroscopy measurements. One important aspect is that there is very little change between these lines recorded from the pure metal and from the oxide. This is because the modifications induced by the

bonding do not involve any of the initial or final wave functions for the M₄₅ edges. In the case of different valence states (that is, change from 3 plus to 4 plus as in Pr compounds) preliminary measurements have shown clear modifications on the M₅-M₄ lines.

In the spectra of Fig. 20, it is clear that, as a consequence of the strongly localized nature of the 4f wave functions in rare earths, the observed lines have to be interpreted in terms of atomic spectra, calculated for triply ionized free atoms. The theoretical work devoted to this problem (Sugar, 1972a, Bonnelle et al., 1974, Bonnelle et al., 1977, Karnatak et al., 1981) can be summarized as follows. The symmetry rule favours transitions of type d → f. A strong repulsive potential barrier allows an easy penetration of the 4f orbitals on the atomic site, but repels the 5f ... εf of higher principal quantum number. A one electron transition such as the 3d → 4f model is insufficient to explain the distribution of the observed fine structures; one has therefore to consider transitions between electron configurations, such as :



Simple cases with LS coupling and a strong spin-orbit term have been calculated and the relative energy positions and oscillator strengths are in good agreement with the observed structures.

N₄₅ edges in rare-earth oxides. (Fig. 23)

For the same specimens, one records in the energy loss range 100 to 200 eV a family of rather characteristic profiles, which can be attributed to the excitation of the 4d_{3/2} and 4d_{5/2} electrons on the rare-earth ions. Some examples are shown in Fig. 23. They are in rather good agreement with edges already recorded in EELS (Trebbia and Colliex, 1973, Ahn and Krivanek, 1982) or in X-ray absorption measurements (Zimkina et al., 1967, Haensel et al., 1970). They are characterized by the existence of one main resonant absorption which lies typically at 10 or 20 eV above the edge position tabulated in photoelectron spectroscopy measurements (see arrows on the spectra). Moreover they display a variety of fine structures -single or double peaks- which do not seem to follow a simple rule. Here again an atomic model following Dehmer et al.(1971) and Sugar (1972b) seems to provide a rather satisfactory description of the observed N₄₅ lines. It considers atomic transitions of type 4d¹⁰4fⁿ → 4d⁹4fⁿ⁺¹ in triply ionized atoms. The main difference with the previous case is that the coulombian and exchange interactions between the 4d hole and the 4f electrons are much stronger than the spin-orbit interaction. Consequently, the multiplet splitting in the final configuration redistributes all final states over a rather large energy domain and prevents one from clearly discriminating the N₄ and N₅ edges. To conclude, the comparison between the 3d → 4f and 4d → 4f transitions in the same rare-earth oxides is very useful. In a single electron model, both transitions would probe the same final level and the relative distribution of near edge intensity would be comparable. Clearly

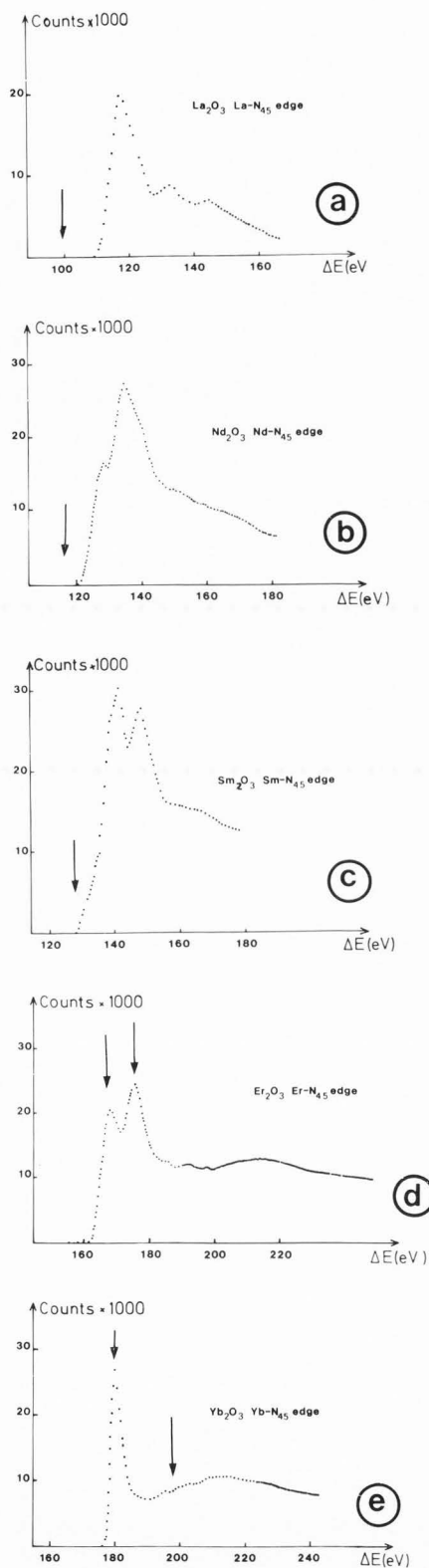


Fig. 23 - The N_{45} edges in rare-earth oxides :
 (a) La_2O_3 ; (b) Nd_2O_3 ; (c) Sm_2O_3 ;
 (d) Er_2O_3 ; (e) Yb_2O_3

this is not the case, and one has to consider transitions in a multielectron system, in which there exist strong intraatomic electron reorganizations around the primary hole.

Conclusion

Edge shape analysis in EELS constitutes an intrinsically powerful technique for probing local chemical, electronic and structural properties from an atomic point of view in the solid. It is therefore highly advisable to push further experimental and theoretical efforts in this direction. The present paper has shown that the task of collecting reference spectra, though still in its infancy, is not impossible. A catalogue of spectra provides a major source of information and in many cases one can begin to compare new edge shapes with a compilation of previously recorded ones on well-defined specimens. Such a systematic approach is also being adopted by the synchrotron radiation community, in the absence of satisfactory theory. Thus comparisons are being pursued of transition metal K-edges in various chemical environments (see for instance Calas and Petiau, 1983, Sayers et al., 1984). On the other hand it is desirable that the availability of high quality experimental spectra further stimulates theoretical work on spectral interpretation, either using the multiscattering approach of the XANES formalism, or using band structure projected DOS calculations.

The potential information derivable from these fine structure studies can be classified according to spectral region as follows (one considers both EELS and X-ray absorption spectra bearing in mind that the second one is more powerful in terms of sensitivity for homogeneous specimens, while the first one has the advantage of studying heterogeneous systems with a typical 10 nm resolution) :

- . edge threshold : information on the valence state or bond covalency for the chemical state of the absorbing atom ; concerning the first atomic shell around this specific site, it can perhaps indicate the symmetry and even its distortion at a particular site. This method should be compared to optical spectroscopy, electron spin resonance or Mossbauer technique.

- . EXAFS (or EXELFS) : deals essentially with properties of the first surrounding shell, giving the co-ordination and particularly the distance between the excited atom and its closest neighbours. Improving the technique should produce information concerning more distant shells. EXELFS is likely to remain of limited application for reasons previously discussed.

- . XANES (or ELNES) : deals more with structural properties at longer distance from the absorbing atom ; that is involving the organisation of the various second, third.. shells in a cluster around the absorbing atom.

Acknowledgements

We want to thank C. Noguera for her illuminative discussions concerning the theoretical background for the interpretation of ELNES and EXELFS structures and L.A. Grunes for his very critical and useful reading of our manuscript.

References

- Ahn C.C., Krivanek O.L. (1982). An Atlas of Electron Energy Loss Spectra. Center for Solid State Science, ASU, Tempe Az. 85287, USA.
- Amusia M.Y. (1974). Manifestation of collective behaviour of electron shells in the process of photo-ionization. In Vacuum UV Radiation Physics, 205-224, Ed. E. Koch, R. Haensel, C. Kunz, Pergamon Vieweg, New York.
- Ashley C., Doniach S. (1975). Theory of Extended X-ray absorption edge fine structure (EXAFS) in crystalline solids. *Phys. Rev.* **B11**, 1279-1288.
- Balzarotti A., Bianconi A., Burattini E., Piacentini M., Strinaki G., Grandolfo M., Habel R. (1974). Soft X-ray electronic transitions from Al-2p level. In Vacuum UV Radiation Physics, 458-461, Ed. E. Koch R. Haensel, C. Kunz, Pergamon. Vieweg, New-York.
- Batson P.E., Craven A.J. (1979). Extended fine structure on the carbon core ionization edge obtained from nanometer sized areas with EELS. *Phys. Rev. Letters*, **42**, 893-897.
- Batson P.E., Gibson J.M., Ferrier R.P. (1980). Structural studies on small areas using STEM. *Journ. of Non-Cryst. Solids*, vol. **35-36**, 525-530. North Holland Publishing Company.
- Bianconi A. (1979). Core excitons and inner well resonances in surface soft X-ray absorption (SSXA) spectra. *Surface Science*, **89**, 41-50.
- Bianconi A. (1981). X-ray absorption Near edge structures (XANES) and their applications to local structure determination. Proceedings of the Daresbury study week-end 1981 (DL/SCI/R17), 11-20. Science & Engineering Research Council, Daresbury, Warrington WA4 4AD (G.B.).
- Bonnelle C., Karnatak R.C., Sugar J. (1974). Photoabsorption in the vicinity of 3d absorption edges of La, La₂O₃ and CeO₂. *Phys. Rev.* **A9**, 1920-1923.
- Bonnelle C., Karnatak R.C., Spector N. (1977). Photoabsorption in the vicinity of 3d edges of Eu and Gd. *J. Phys.* **B10**, 795-801.
- Brown L.M., Colliex C., Gasgnier M. (1984). Fine structure in EELS from rare earth sesquioxides thin films. ICXOM Conference, Toulouse. *J. Physique C2*, 433-436. Les Editions de Physique, Orsay.
- Calas G., Petiau J. (1983). Coordination of iron in oxide glasses through high resolution K-edge spectra : information from the pre-edge. *Solid State Communication Vol.* **48**, 625-629.
- Caro P.E. (1968). OM₄ tetrahedra linkages and the cationic group (MO)_n⁺ in rare-earth oxides and oxyalts. *J. Less Common Metals*, **16**, 367-377.
- Citrin P.H., Rowe J.E., Christman S.B. (1976). Interatomic Auger transitions in ionic compounds. *Phys. Rev.* **B14**, 2642-2658.
- Colliex C., Jouffrey B. (1972). Inelastic scattering of electrons in solids by core atomic level excitations. Energy loss spectra. *Phil. Mag.* **25**, 491-511.
- Colliex C., Cosslett V.E., Leapman R.D., Trebbia P. (1976). Contribution of EELS to the development of analytical electron microscopy. *Ultramicroscopy* **1**, 301-315.
- Colliex C., Jeanguillaume C., Trebbia P. (1981). Quantitative local microanalysis with EELS. In *Microprobe analysis of biological systems*, 251-271, Eds. T.E. Hutchinson, A.P. Somlyo, Acad. Press, London, N.Y.
- Colliex C., Treacy M.M.J. (1983). The Scanning Transmission Electron Microscope (STEM). In *Microscopie électronique en science des matériaux*, Ecole d'été du CNRS à Bombanes (1981), pages 391-424. Editions du CNRS (1983).
- Colliex C. (1982). Electron energy loss analysis in materials science. 10th International Congress on Electron Microscopy, Hamburg. In "Electron Microscopy 1982", vol. 1, pp. 159-166. ed. The Congress Organizing Committee.
- Colliex C., Trebbia P. (1982). Performance and application of EELS in STEM. *Ultramicroscopy*, **9**, 259-266.
- Colliex C., Mory C. (1983). Quantitative aspects of STEM. In *Quantitative Electron Microscopy*, 25, 149-216. Ed. J.N. Chapman and A.J. Craven, published by SUSSP, Edinburgh University - Physics Department King's Buildings, Mayfield Road - Edinburgh.
- Colliex C. (1984a). Electron energy loss spectroscopy in the electron microscope. *Adv. in Optical and Electron Microscopy*, **9**, 65-177. Eds. R. Barer and V.E. Cosslett, Academic Press, London, N.Y.
- Colliex C. (1984b). Present capabilities and limits of chemical analysis in the electron microscope. In *Electron Microscopy I (1984)*, 349-363. Proceedings of the 8th European Congress on Electron Microscopy. (Budapest, August 13-18, 1984). Ed. A. Csányi, P. Röhlich and D. Szabo. Published by the Programme Committee of the 8th EUREM, Budapest, P.O. Box 32, H-1361 Hungary.
- Csillag S., Johnson D.E., Stern E.A. (1981). Extended energy loss fine structure studies in an electron microscope. In "EXAFS Spectroscopy - Techniques and Applications". Ed. Teo B.K. and Joy D.C., pp. 241-254, Plenum Press, New York, London.
- Dehmer J.L., Starace A.F., Fano U., Sugar J., Cooper J.W. (1971). Raising of Discrete Levels into the Far Continuum. *Phys. Rev. Lett.* **26**, 1521-1525.
- Disko M.M., Krivanek O.L., Rez P. (1982). Orientation dependent extended fine structure in EELS. *Phys. Rev.* **B25**, 4252-4255.
- Disko M.M., Spence J.C.H., Sankey O.F. (1984). Site symmetry information in Electron Energy Loss Near Edge Fine Structure. *Proc. 30th International Congress of Crystallography, Hamburg*, C.467, ed. U. Bonze, Dortmund.
- Dorignac D., Maclachlan M.E.C., Jouffrey B. (1979). Low-noise boron supports for high resolution electron microscopy. *Ultramicroscopy*, **4**, 85-89.
- Dow J.D. (1974). X-ray edges : broadening mechanisms, selection rules, sum rules, compatibility relationship and orthogonality catastrophes. In *Vacuum UV Radiation Physics*, pp. 649-661, ed. E. Koch, R. Haensel, C. Kunz, Pergamon Vieweg, New-York.
- Durham P.J., Pendry J.B., Hodges C.H. (1981). XANES: determination of bond angles and multi-atom correlations in ordered and disordered systems. *Solid State Commun.* **38**, 159-162.

- Durham P.J., Pendry B., Hodges C.H. (1982). Calculation of X-ray absorption near-edge structure, XANES. *Computer Physics Commun.* 25, 193-205.
- Egerton R.F., Whelan M.J. (1974). The electron energy loss spectrum and band structure of diamond. *Phil. Mag.* 30, 739-748.
- Egerton R.F. (1975). Inelastic scattering of 80 keV e⁻ in amorphous carbon. *Phil. Mag.* 31, 199-215.
- Egerton R.F. (1983). Electron Energy Loss Spectroscopy. In *Quantitative Electron Microscopy* 25, 273-304. Ed. J.N. Chapman and A.J. Craven. Published by SUSSP. Edinburgh University. Physics Department. King's Buildings, Mayfield Road, Edinburgh.
- Egerton R.F. (1984). Quantitative Microanalysis by EELS: the Current Status. *Scanning Electron Microsc.* 1984; II: 505-512.
- Fischer D.W. (1971). Soft X-ray band spectra and molecular orbital structure of Cr₂O₃, CrO₃, CrO₄²⁻, Cr₂O₇²⁻. *J. Phys. Chem. Solids*, 32, 2455-2480.
- Friedel J. (1954). Electronic structure of primary solid solutions in metals. *Adv. Phys.* 3, 446-507.
- Fuggle J.C. (1981). High resolution Auger spectroscopy of solids and surfaces in *Electron Spectroscopy: theory, techniques and applications*, vol. 4, 85-152. Eds. C.R. Brundle and A.D. Baker, Academic Press, N.Y.
- Gasgnier M. (1980). Rare-earth metals, rare-earth hydrides and rare-earth oxides as thin films. A critical review. *Phys. Stat. Sol. (a)* 57, 11-57.
- Grunes L.A. (1982). A study of core excitation spectra in 3d transition metals and oxides by EELS and X-ray absorption spectroscopy. Thesis, Cornell University, Ithaca, N.Y.
- Grunes L.A., Leapman R.D., Wilker C.N., Hoffmann R., Kunz A.B. (1982). Oxygen K near edge fine structure: an electron energy loss investigation with comparison to new theory for selected 3d transition metal oxides. *Phys. Rev.* B25, 7157-7173.
- Grunes L.A. (1983). Study of the K edges of 3d transition metals in pure and oxide form by X-ray absorption spectroscopy. *Phys. Rev.* B27, 2111-2131.
- Haensel R., Rabe P., Sonntag B. (1970). Optical absorption of cerium, cerium oxide, praseodymium, praseodymium oxide, neodymium oxide and samarium in the extreme ultraviolet. *Solid State Commun.* 8, 1845-1848.
- Hayes T.M., Boyce J.B. (1982). Extended X-ray absorption fine structure spectroscopy. *Solid State Physics*, 37, 173-348.
- Heine V. (1980). Electronic structure from the point of view of the local atomic environment. *Solid State Physics*, 35, 1-126.
- Hitchcock A.P., Brion C.E. (1980). K-shell excitation spectra of CO, N₂ and O₂. *J. Electron. Spectr. and Related Phenomena*, 18, 1-21.
- Hosoi J., Oikawa T., Inoue M., Matsui Y., Endo T. (1982). Study of boron nitride by EELS. *J. Electron. Spectr. and Related Phenomena*, 27, 243-254.
- Isaacson M. (1979). EELS within the microscope. Where are we? In *"Microbeam Analysis in Biology"*, Eds. Lechene C.P. and Warner R.R., 53-61, Academic Press, New York.
- Jeanguillaume C., Krivanek O.L., Colliex C. (1982). Optimum design and use of homogeneous magnetic field spectrometers in EELS. *Inst. Phys. Conf. Ser.* 61, 189-192.
- Johnson D.W., Spence J.C. (1974). Determination of the single scattering probability distribution from plural scattering data. *J. Phys.* D7, 771-780.
- Karnatak R.C., Esteva J.M., Connerade J.P. (1981). On the profiles and linewidths of the 3d → 4f transitions in the lanthanides. *J. Phys.* B14, 4747-4754.
- Kincaid B.M., Meixner A.E., Platzman P.M. (1978). Carbon K-edge in graphite measured using EELS. *Phys. Rev. Lett.* 40, 1296-1299.
- Krivanek O.L., Swann P.R. (1981). An advanced electron energy loss spectrometer. In *"Quantitative Microanalysis with High Spatial Resolution"*, pp. 136-140, Ed. The Metals Society, London.
- Krivanek O.L. (1982). Recent results in EELS. 10th International Congress on Electron Microscopy. Hamburg. In *"Electron Microscopy 1982"*, Vol I, pp. 167-172. Ed. The Congress Organizing Committee.
- Lander J.J. (1953). Auger peaks in the energy spectra of secondary electrons from various materials. *Phys. Rev.* 91, 1382-1387.
- Laüger K. (1971). About the influence of binding state and crystalline structure about the K_{α1,2}-X-Ray spectrum. *J. Phys. Chem. Solids*, 32, 609-622.
- Leapman R.D., Cosslett V.E. (1976). Extended fine structure above the X-ray edge in EELS. *J. Phys.* D9, L-29-32.
- Leapman R.D., Grunes L.A., Fejes P.L., Silcox J. (1981). Extended core edge fine structure in electron energy loss spectra. In *"EXAFS spectroscopy techniques and applications"*. Ed. Teo B.K. and Joy D.C., pp. 217-239, Plenum Press, New York, London.
- Leapman R.D. (1982). EXELFS spectroscopy of amorphous materials. In *"Microbeam analysis 1982"*, pp. 111-117. Ed. K.F.J. Henrich, San Francisco Press.
- Leapman R.D., Grunes L.A., Fejes P.L. (1982). Study of the L₂₃ edges in the 3d transition metal and their oxides by electron-energy loss spectroscopy with comparisons to theory. *Phys. Rev.* B26, 614-635.
- Leapman R.D., Fejes P.L., Silcox J. (1983). Orientation dependence of core edges from anisotropic materials determined by inelastic scattering of fast electrons. *Phys. Rev.* B28, 2361-2373.
- Lee P.A., Pendry J.B. (1975). Theory of the extended X-ray absorption fine structure. *Phys. Rev.* B11, 2795-2811.

- Lee P.A., Citrin P.H., Eisenberger P., Kincaid B.M. (1981). Extended X-ray absorption fine structure. Its strengths and limitations as a structural tool. *Reviews of Modern Physics*, vol. 53, 769-806.
- Madden H.H. (1983). Auger lineshape analysis. *Surface Science*, 126, 80-100.
- Mahan G.D. (1974). Edge singularities in X-ray spectra. In "Vacuum UV Radiation Physics", 635-647, ed. E. Koch, R. Haensel, C. Kunz, Pergamon Vieweg, New York.
- Mele E.J., Ritsko J.J. (1979). Fermi level lowering and the core exciton spectrum of intercalated graphite. *Phys. Rev. Lett.* 43, 68-71.
- Nakhmanson M.S., Smirnov V.P. (1972). Band structure and density of states in hexagonal BN. *Sov. Phys. Solid State* 13, 2763-2768.
- Noguera C. (1981). Problèmes de structure électronique liés à la photoexcitation d'un atome en surface et en volume dans un métal. Thèse, Orsay, Université Paris-Sud, Orsay, France.
- Pantelides S.T., Mickish D.J., Kunz A.B. (1974). Electronic structure and properties of magnesium oxide. *Phys. Rev.* B10, 5203-5212.
- Pittel B., Schwartz W.H.E., Rabe P., Friedrich H., Sonntag B. (1979). Overlapping core to valence-core to Rydberg transitions and resonances in the XUV spectra of SiF₄. Desy Report, SR 79/16. Deutsches Elektronen synchrotron, Notkesstrasse 85, Hamburg 52.
- Ritsko J.J., Schnatterly S.E., Gibbons P.C. (1974). Simple calculation of L_{II,III} absorption spectra of Na, Al and Si. *Phys. Rev. Lett.* 32, 671-674.
- Sayers D.E., Stern E.A., Lytle F.W. (1971). New techniques for investigating non crystalline structures. Fourier analysis of EXAFS. *Phys. Rev. Lett.* 27, 1204-1207.
- Sayers D.E., Theil E.C., Rennick F.J. (1984). A distinct environment for iron III in the complex with horse spleen apoferritin observed by X-ray absorption spectroscopy. *J. Biol. Chem.*, in press.
- Stephens A.P., Brown L.M. (1981). EXELFS in graphitic boron nitride. In "Quantitative Microanalysis with High spatial resolution, 152-158. Ed. The Metals Society, London.
- Sugar J. (1972a). Interpretation of photoabsorption in the vicinity of 3d edges in La, Er and Tm. *Phys. Rev.* A6, 1764-1767.
- Sugar J. (1972b). Potential barrier effects in Photoabsorption. II) Interpretation of photoabsorption resonances in lanthanide metals at the 4d electron threshold. *Phys. Rev.* B5, 1785-1792.
- Swanson N., Powell C.J. (1968). Excitation of L-shell electrons in Al and Al₂O₃ by 20 keV electrons. *Phys. Rev.* 167, 592-600.
- Swyt C.R., Leapman R.D. (1982). Plural scattering in EELS microanalysis. *Scanning Electron Microscopy 1982* ; I:73-82.
- Taftø J., Zhu J. (1982). ELNES, a potential technique in the studies of local atomic arrangements. *Ultramicroscopy* 9, 349-354.
- Trebbia P., Colliex C. (1973). Study of the excitation of 4d electrons in rare-earth metals by inelastic scattering of a high energy electron beam. *Phys. Stat. Sol.(b)* 58, 523-532.
- Wendin G. (1974). Effects of localized excitations on the dynamic response of atoms and solids. In "Vacuum UV Radiation Physics 635-647. Ed. E. Koch, R. Haensel, C. Kunz, Pergamon Vieweg, New York.
- Zaluzec N.J. (1982). An electron energy loss spectral library. *Ultramicroscopy* 9, 319-324.
- Zimkina T.M., Fomichev V.A., Gribovskii S.A., Zhukova I.I. (1967). Anomalies in the character of the X-ray absorption of rare-earth elements of the lanthanide group. *Sov. Phys. Solid State*, 9, 1128-1130.

Discussion with Reviewers

R.D. Leapman : It has been reported that micro-analysis of normally radiation resistant materials in STEM at a 1 nm resolution can result in mass loss. To what extent will information from fine structure in materials samples be limited by beam damage ?

Authors : There is no single well defined answer to this question. The recording of a useful spectrum for fine structure analysis requires typically 100 to 500 s with our instrument (incident beam $\approx 10^{-10}$ A). The relevant doses are enormous, depending on the size of the analysed area ; they are in the range 10^7-10^8 e⁻/Å² for a typical 100 Å lateral dimension. Of course such numbers prevent from extracting this type of information in beam-sensitive materials. Concerning current situations in materials science, we can compare these values to the critical dose that we have estimated for the beam-induced desorption of oxygen from dislocation cores in pure germanium (typically 10^6 e⁻/Å²) - see A. Bourret, C. Colliex, P. Trebbia (1983) *J. Physique - Lettres* 44, 33-37 -. It constituted however one problem for which beam damage was rather intense, as compared to many other micro-analytical cases which we investigated in this field.

R.D. Leapman : Could the authors give some possible applications in physics or materials science where determination of electronic structure or chemical bonding might produce useful information in the dedicated STEM ?

J.C.H. Spence. I feel strongly that a statement giving more historical perspective must be added. XANES is not a new field but has been studied since the 1920's by eminent scientists such as Kossel (*Z. Phys.* 1, 119 (1920)), Kronig ((*Z. Phys.* 70, p. 317 (1931))) and Mott (*Phil. Mag.* 40, p. 1260 (1949)). In general I feel that this review paints an overly optimistic picture, and would be improved by the addition of a comment to the effect that sixty years work in the XANES field is now just beginning to show very limited success in simple cases (note that the Pendry method fails for semiconductors or other strongly covalent materials because of the muffin-tin approximation), and that, since ELNES interpretation is further complicated by the effects of multiple inelastic (e.g. plasmon satellites) and elastic (i.e. fast electron diffraction) scattering, it is likely to be some time before quantitative agreement between ELNES theory and experiment can be expected.

Authors : These question and comment raise the problem of the field of application of the method, which is a real question though this tutorial

paper was more intended to cover the fundamental study of this refined type of information. Some arguments have been given in the text concerning problems at interfaces for instance ; it is clear that a limitation in these highly localized situations will lie in the beam dose requirements already discussed. We are more confident in a rather near future use of these ELNES features in mineralogical or chemistry problems for which a typical lateral size of 100 Å is sufficient. There exist problems concerning the reactivity of thin foils, for instance Praseodymium which lead to valence and structural fluctuations appearing in complex unknown phases, for which an average grain size is typically a few hundred Å. Another example concerns amorphous oxide glass (study of the valence state, coordination geometry). In such cases, the analysis of fine structures, at the edge and of XANES type, would be very useful.

R.F. Egerton : If Fig. 11 is to be useful for solids, one would need some way of determining the boundary E_0 between excitation to bound states and ionization to the continuum. How might this be achieved ?

Authors : This question raises comments on two levels : what is the real meaning of this curve in the case of molecules ? How far can it be applied for solid system ? Back to the first point, we can refer to Cadioli F., Pincelli U., Tosatti E., Fano U., Dehmer J.L. (1972). Chem. Phys. Lett. 17, 15, for a first discussion of the concept of an effective potential barrier acting on the photoelectrons excited from a central atom surrounded by two or more electronegative atoms. This effect is revealed because photoelectrons escaping with energies of the order of 10 eV seem unable to pass freely through the electronegative atoms on the periphery of the molecule. Consequently, the final available states are classified into "inner well" states localized in the space enclosed by the electronegative atoms and "outer well" states localized outside of these atoms for both the continuum and discrete part of the spectrum. The relationship shown in Fig. 11 originates from a work by Brown F.C., Bachrach R.Z. and Bianconi A. (1978). Chem. Phys. Letters 54, 425, which has revealed strong chemical shifts of the first excited states at the carbon K-edge with increasing fluorination of the CH_4 molecule. These shifts closely follow ESCA binding energy shifts and exceed 10 eV in CF_4 . Consequently Bianconi (1981) uses the empirical relationship between the chemical shift of E_0 and the chemical shift of the first peak at the edge to estimate in the absence of ESCA data a value of E_0 in another molecular case, from an absorption spectrum (or EELS spectrum) where no characteristic feature appears at E_0 . This binding energy increases with the effective positive charge on the C atom and this is the proposed solution to obtain information on it.

Concerning the extension to solids, a simple remark can be made. The basic idea is that, to determine the properties of the excited site in a large complex molecule, one has to compare the XANES structure of this selected atom with the XANES of the same atom in simple chemical compounds

where it is known to occupy similar sites. This is a consequence of the assumption that the spectrum is sensitive only to the local structure. In a few compounds for which the "molecular environment" seems important, there are experimental data supporting this idea. For instance one can quote the nice similarity between the L_{23} edge profile of Si in SiF_4 gas and solid as shown by Pittel et al. (1979). Moreover the L_3 -XANES of SiO_2 is also very similar to the XANES of SiF_4 , indicating the prominence of the structural unit SiO_4 in the solid SiO_2 .

The present comment aims more generally to point out the importance, in a few solid compounds, of the molecular potential due to the molecular "cage" defined by the first shell of ligands, the effects of which have been clearly discussed by Kutzler F.W., Natoli C.R., Misemer D.K., Doniach S. Hodgson K.O. (1980), J. Chem. Phys. 73, 3274-3288.

R.F. Egerton : Can you explain why (in MgO) states at the bottom of the conduction band have an enhanced weight on the oxygen atoms, i.e. what assumption does this make about the bonding ?

Authors : The case of MgO is very different from the type of solids discussed in the answer to the preceding question. It constitutes a typical example for which the solid state description and the DOS concept are of fundamental importance to understand the shape of the ionization edge. To compare with the above discussion of the ionization energy E_0 ; the relevant parameter is now the energy of the core level with respect to the bottom of the conduction band. In insulators, such as MgO, it can be estimated theoretically, such as done by Pantelides et al. (1974), as the combination of the Hartree-Fock ground state modified by the self energies of the electron in the conduction band and of the hole on the core level. It can also be measured from X-ray emission data or ESCA experiments, both of which provide an accurate value for the position of the top of the valence band relative to the core level. One has then to add an energy equal to the band gap (7.8 eV in MgO). When following this latter approach, one estimates the threshold energy at ≈ 535 eV for the oxygen K-edge and ≈ 1307.5 eV for the magnesium K-edge. The peaks labeled as "a" in Fig. 15 are located below this value.

Coming back to the interpretation in terms of local DOS suggested in the text, it would mean that the antibonding p-states at the bottom of the conduction band would be more abundant on the anion (oxygen) site than on the cation (magnesium) site, which seems in contradiction with the simple ionic models of charge transfer between the O^{2-} and Mg^{2+} ions.

Consequently, for these two reasons, we feel that MgO constitutes a clear example in which core-excitations are of importance. A very complete discussion has been devoted by Pantelides S. (1975), Phys. Rev. B11, 2391 to electronic excitation energies and soft X-ray absorption spectra of alkali halides. He points out the fact that electron-hole interactions are so large in case of excitations of the cation core electron, that such a spectrum is nearly entirely excitonic in nature. It is not quite so in the case of excitations of the anion, where electron-hole attraction is more effectively

screened. How far these remarks can be used to understand the intensity behaviour of ELNES structures on Mg and O-K edges, is still open to discussion.

L.A. Grunes. For comparisons to theory, it is important to present experimental data recorded at high energy resolution, high signal-to-noise ratio and with accuracy in the absolute energy scale. Although you report ELNES energies to the nearest 0.010 eV, the magnetic sector spectrometer employed by you has no absolute calibration that I know of, and may be non-linear in its energy dispersion. Hence merely comparing data from standard specimens measured by other means would not establish the absolute energies of your spectral features to any better than, say, 1.0 eV. Besides the energy resolution of your microscope/spectrometer is only about 1 eV. It seems to me that quantitative studies of core near edge structure are best done using synchrotron monochromators, such as the one at SSRL (Stanford) which provide superior signal-to-noise, energy resolution, and energy calibration. The one important advantage of a STEM over a synchrotron facility lies in its ability to analyze extremely small lateral specimen areas, e.g. small particles or interfaces. Have you attempted any such studies?

Authors : When comparing features on the same energy loss recording over a reduced energy range around the edge (typically 0.2 eV per channel), the whole stability of the system is sufficient so that we can claim accuracies of ± 0.2 eV on energy differences (see tables). On the contrary, as there is no absolute calibration on the employed magnetic sector spectrometer, we are obliged to compare the energy position of edges of interest with known features such as the π^{**} peak of the contamination carbon K-edge. Consequently our absolute energy scale accuracy is only of the order of ± 1 eV.

J.C.H. Spence : Could the authors comment on the conditions for the failure of the dipole approximation in ELNES? Is an experimental test available?

Authors : The failure of the dipole approximation can be discussed from the following equation, corresponding to the probability of transition between the fundamental state $|0\rangle$ and the excited state $|n\rangle$:

$$P(\Delta E, \vec{q}) \propto \frac{1}{q^4} |\langle n | \exp(i\vec{q} \cdot \vec{r}) | 0 \rangle|^2 = \frac{1}{q^4} |\langle n | 1 + iq(\vec{\epsilon}_q \cdot \vec{r}) - \frac{q^2}{2} (\vec{\epsilon}_q \cdot \vec{r})^2 | 0 \rangle|^2$$

with $\vec{\epsilon}_q$ a unit vector along the momentum change \vec{q} .

The dipole term dominates at small q and is responsible for the optical ($\Delta l = \pm 1$) transitions generally observed. This contribution falls in angle as $1/q^2$. For large angle the next term with no intensity dependence in q , becomes important, involving monopole ($\Delta l = 0$) or quadrupole ($\Delta l = 2$) transitions. They begin to be detected when $q \approx 1/r_c$ where r_c is the mean radius of the excited orbital. For instance $r_c = 0.09 \text{ \AA}$ for the oxygen 1s electron at 532 eV. The required value of q for detecting non dipole transition is $> 10 \text{ \AA}^{-1}$ which corresponds to scattering angles far greater than the 25 mrad of our collection angle. Some non-dipole effects could however be detected for N₄₅

edges in Ln for instance, at large angles of scattering. We did not consider this effect in detail.

J.C.H. Spence : XANES calculations and experiments are often performed for a single polarization direction. Are not comparisons with ELNES complicated by the fact that if say, a 25 mrad collection aperture is used in ELNES an average over all "polarization" would be required? The large beam divergence needed to obtain a 3 Å probe may further contribute to this effect.

Authors : Our instrumental values of illumination angle are far too large to probe orientation-dependent fine structures in ELNES, for anisotropic materials such as BN or graphite, which require typical angular widths below 1 mrad. Consequently the type of information that we obtained is an "average" over all polarizations, as you mention. The comparison of our data with those obtained by Leapman, Fejes and Silcox (1983) is a clear evidence of the loss of information, in our STEM geometry which is more dedicated to high spatial resolution. In this field, one can make also reference to the recent work of Maslen V.W. and Rossouw C.J. (1983) Phil. Mag. A47, 119. They have derived a full calculation of the scattering kinematics involved in the collision of a fast electron with a K-shell electron from an atom, which enables to study the angular dependence of the ejected electron intensity. This approach is fully relevant to investigate the angular dependence of EXELFS and ELNES fine structures. These authors point out that with collection angles above 10 mrad, these fine structures would be rather insensitive to crystal orientation.

J.C.H. Spence : Have the authors observed changes in the ELNES as the probe is moved within a single unit cell? If so, how does this complicate the interpretation?

Authors : This would constitute the type of extreme performance that you can hope for a dedicated STEM. It is evident that such observation could only be made with large cell materials, such as the Ba-0.6 Al₂O₃ crystal on which you have worked to record changes in relative intensity between Ba-M₄₅ edge and O-K edge (Spence J.C.H., Lynch J., (1982), Ultramicroscopy 9, 267). The requirement in dose, already mentioned, has prevented us to undertake such experiments when the smallest probe size (and consequently highest primary doses) is required.

J.C.H. Spence : Is there an experimental test which can be used to ensure that multiple elastic scattering effects are negligible?

Authors : We think that this question refers to the problem of inelastic electron diffraction in crystals such as discussed recently by Maslen V.W. and Rossouw C.J. (1984), Phil. Mag. A49, 735 and 743 and in the literature quoted therein. We must confess that we could not yet consider in detail how the fact that the primary electron propagates as a Bloch wave through the crystal may modify the energy loss intensity distribution near an edge, when using our geometrical conditions. Consequently we leave this question temporarily unanswered.